Future projections of rain-on-snow events and their spatiotemporal distribution across the Fraser River Basin, British Columbia, Canada

by

Santosh Neupane

A thesis

presented to the University of Waterloo

in fulfillment of the

thesis requirement for the degree of

Master of Science

in

Geography (Water)

Waterloo, Ontario, Canada, 2019

© Santosh Neupane 2019

Author's Declaration

I hereby declare that I am the sole author of this thesis. This is a true copy of the thesis including the required final revisions, as accepted by my examiners.

I am aware that my thesis may be made electronically available to the public.

Abstract

This study analyzes the projected changes of rain-on-snow (ROS) event characteristics (frequency, mechanism and runoff) for the future (2020 – 2099) period with respect to the historical period (1970 – 1999) over the Fraser River Basin (FRB), British Columbia, Canada. The ROS-induced runoff contributes more than half of the total runoff in FRB during the cold season. Simulated snow water equivalent (SWE) and spatial runoff from the Variable Infiltration Capacity (VIC) model are used to estimate the spatial distribution and change of ROS events, based on a multi-model ensemble of climate forcing data following the RCP 8.5 emissions scenario. Prior to assessing the future evolution, VIC is validated by comparing the historical and observed frequency of ROS events seasonally for the period 1970 – 1999. This comparison indicates a similar spatial pattern and seasonal trend in ROS across the basin, but VIC produces about 2-4 times the number of observed ROS events. Future ROS characteristics are assessed in four different elevational bands, and different responses of ROS evolution are found at different elevations. ROS events are projected to decline rapidly in the lowest elevation zone, and to increase in higher elevation zones as a function of changes to the environmental lapse rate. Specifically, wintertime ROS frequency is expected to increase rapidly in higher elevation zones as cold temperatures there produce a consistent snowpack, combined with an increasing frequency of rainfall events driven by projected warming. The correlation between changes of ROS, rainfall, temperature and snow water equivalent (SWE) indicates that increasing temperature drives the decline in future ROS at the lower elevation. In contrast, both temperature and rainfall enhance the positive ROS trend in higher elevation zones. Despite the ongoing warming phenomenon is continuously shrinking snowpack, future ROS evolution is not limited by available snow on the ground and follows an increasing trend until the end of the 21st century. The ROS-induced surface runoff during the cold season is expected to increase in the future, with greater increases at higher elevation. The novel contribution of this research is to provide projections, with an estimate of their uncertainty, of the change in seasonality of streamflow in the FRB, particularly during the winter-spring snowmelt period. The results show that ROS events require careful consideration for future planning in surface water resources management in snowmelt-dominated hydrologic regimes.

Acknowledgments

I would like to thank my parents Ram and Basanta as well as my beloved wife for supporting during this program by encouraging me through motivations and inspirations to accomplish the graduate study. I would also like to thank my advisor Dr. Chris Fletcher who has supported and directed me to achieve success. Additionally, I would like to thank other members of the science community including Dr. Stephen Dery, Dr. Siraj UI Islam for providing data and feedbacks during the data analysis period, and Dr. Mike Stone and Stephanie Shifflett for providing valuable feedback throughout the defense process. I would also like to extend thanks to my lab-mates who supported me to accomplish my research analysis.

Table of Contents

Author's Declaration ---- i

Abstract ---- ii

Acknowledgments ---- iii

List of Figures ---- vi

Chapter 1: Introduction ---- 1

1.1 Climate Change and Cold Region Environment ---- 1

1.1.1 Background ---- 1

1.1.2 Rain on Snow ---- 2

1.1.3 Study Area and climatology ---- 5

1.2 Aims and Objectives ---- 8

1.3 Thesis structure ---- 8

Chapter 2: Data and Methodology ---- 9

2.1 Model Simulations ---- 9

a) Variable Infiltration Capacity (VIC) model Description ---- 9

b) Boundary Conditions ---- 11

2.2 Data Sources ---- 12

2.3 Quantifying rain-on-snow events ---- 13

a) Classification of ROS Days ---- 14

Chapter 3: Results ---- 16

3.1 Seasonal Climate ---- 16

3.1.1 Observed Rainfall Climatology ---- 16

3.1.2 Observed Temperature Climatology ---- 18

3.2 Temperature and Precipitation Change ---- 19

3.2.1 Temperature Change ---- 19

3.2.2 Precipitation Change ---- 21

3.3 Observed, Historical and Scenario ROS Events ---- 24

3.4 Future Projected Changes of ROS Events ---- 27

a) Elevation range 0 – 500 m ---- 27

b) Elevation range 501 – 1000 m ---- 28

c) Elevation range 1001 – 1500 m ---- 29
d) Elevation range 1501 m and above ---- 29
3.5 Evaluation of ROS Events Simulation ---- 30
a) Elevation range 0 - 500 m ---- 30
b) Elevation range 501-1000 m ---- 31
c) Elevation 1001 -1500 m ---- 32
d) Elevation 1501 m and above ---- 33
3.6 ROS-Induced Runoff Changes ---- 34
Chapter 4: Discussion ---- 38
4.1 Future ROS Changes ---- 38
4.2 The mechanism driving future ROS evolution ---- 39
4.3 ROS Responses to Runoff ---- 40
Chapter 5: Conclusion ---- 42
5.1 Summary ---- 42
References ---- 44
Appendix ---- 52

List of Figures

Figure 1: Digital elevation map of the FRB with major sub-basins: Quesnel (QU), Chilko (CH), Thompson–Nicola (TN), Upper Fraser with a major outlet for FRB at Hope with a red dot..... 6

Figure 2: Spatial variability of the 30-year (1981–2010) mean annual temperature (℃) in panel (a) and mean annual precipitation (mm/year) in panel (b) for the Fraser River Basin based on CANGRID data from Natural Resources Canada. 7

Figure 3: Schematic of the VIC model with the mosaic representation of vegetation coverage.... 9

Figure 4: Schematic of VIC network routing models. 10

Figure 5: CMIP5 multi-model simulated time series from 1950 to 2100 for change in global annual mean surface temperature relative to 1986-2005. The time series of the projections and a measure of uncertainty (shading) are shown for scenarios RCP2.6 (blue) and RCP 8.5 (red) and the black (gray shading) is the modelled historical evolution using historical reconstructed forcing (observed GHG, aerosol forcing and natural climate forcing). 12

Figure 6: Observed Seasonal (Winter (DJF), Spring (MAM), Summer (JJA) and Fall (SON)) Precipitation of the Fraser River Basin for 1970 to 1999 based on CANGRID data from Natural Resources Canada 17

Figure 7: Observed Mean Seasonal (DJF, MAM, JJA, SON) Temperature of Fraser Basin for 1970 to 1999 based on CANGRID data from Natural Resources Canada 18

Figure 8: Average temperature distribution in Fraser River Basin presented in multidecadal (T1=2020-2039, T2=2040-2059, T3=2060-2079, and T4=2080-2099), seasonal (winter(DJF), spring (MAM), summer (JJA), and fall (SON)) in different elevation zones ((a)=0-500 m, (b)=501-1000 m, (c)=1001-1500 m and (d)=1500 & above m). Each boxplot length represents multi-model uncertainty and color indicates the season 19

Figure 9: Minimum temperature density historical (1970-99) period for the different projection period (1970-99, 2020-39, 2040-59, 2060-79 and 2080-99) in FRB with the threshold to filter snow (<-0.5° c), rain (>1.5° C) and mixed type between these two thresholds..... 21

Figure 10: Climate change response to annual precipitation changes (scenario period: 2070-99 & historical period: 1970-99 in Fraser basin with the multi-model agreement (80%) to indicate the model agreeing on the change signal 22

Figure 11: Precipitation phase changes in the future with the multi-model agreement (80%) to indicate the sign of future change 23

Figure 12: Rainfall distribution in Fraser Basin presented in multidecadal (T1=2020-2039, T2=2040-2059, T3=2060-2079, and T4=2080-2099) and seasonal (winter(DJF), spring (MAM), summer (JJA), and fall (SON) in different elevation zones ((a)=< 500 m, (b)=501-1000 m, (c)=1001-1500 m and (d)= > 1501 m). Each boxplot length represents multi-model uncertainty and color indicates the season. 24

Figure 13: Annual ROS events of the observed (a), historical (b) and projected change in scenario (c). Panel (b) and (c) are MME with the multi-model agreement (80%) indicating the sign of future changes in panel (c) 25

Figure 14: Comparison of the historical (top row) and scenario (bottom row) ROS events in the Fraser River Basin for different seasons (winter (DJF), spring (MAM), summer (JJA), and fall (SON) 26

Figure 15: ROS distribution in Fraser Basin presented in multidecadal (T1=2020-2039, T2=2040-2059, T3=2060-2079, and T4=2080-2099), seasonal (DJF, MAM, JJA, and SON) and altitudinal distribution ((a)=0-500 m, (b)=501-1000 m, (c)=1001-1500 m and (d)=1500 & above m). Each boxplot length represents multi-model uncertainty and color indicates the season. 28

Figure 16: The association between projected change of ROS (dROS), Rainfall (dRainfall), Temperature (dTAS) and SWE (dSWE) in the elevation range of 0-500 m. Each circle represents one model projection, and the circle color indicates the time period. 30

Chapter 1: Introduction

1.1 Climate Change and Cold Region Environment

1.1.1 Background

The global climate system is “extremely likely” warming since the mid-twentieth century due to anthropogenic greenhouse gas (GHG) emission and the trend in recent decades is eventually contributing more positive feedback on the earth's climate system (IPCC, 2014). The earth climate has been changing in response to anthropogenic GHG emissions since the industrial revolution. Among different impacts on the earth’s sustaining system, the changes in the climate system have a direct impact on the hydrologic cycle as it affects the flow regime, water resident time, etc. The impact on the hydrologic regime is more aggressive in the high latitude region typically associated with the precipitation phase change affecting the physical properties of the snowpack (Singh, Spitzbart, Hübl, & Weinmeister, 1997). The precipitation phase change can cause a series of impacts on the hydrologic regime on a regional scale such as the change in peak flow, flood frequencies and flood peaking time etc. Recent hydro-climatic trends observed in western North America has been affected by regional climate change (Barnett et al., 2008; Bonfils et al., 2008; Pierce et al., 2008) and the characteristics of snow-hydrology of the North American hydrologic regime has been affected with accelerating earlier spring melt and subsequently decreasing late spring and summer base flow (Déry et al., 2009; Fleming & Weber, 2012; Hatcher & Jones, 2013; Bawden, Linton, Burn, & Prowse, 2014). Further, the warmer air temperature in future climate leads to an increase in the rainfall portion in the total precipitation even in cold months extending mid and high-latitude regions of the northern hemisphere (Jeong & Sushama, 2017a). The tendency of rapid warm in regional temperature and increase in precipitation has directly affected the regional hydrologic regime (Shrestha, Schnorbus, Werner, & Berland, 2012; M. A. Schnorbus & Cannon, 2014; M. Schnorbus, Werner, & Bennett, 2014) in this region. The anticipated increase of rainfall in the winter season in snow-hydrologic regime could have various implications in the ecosystem including early shifting of snowmelt flooding events. In general practices, spring snowmelt floods are stored in reservoirs to maintain minimum flow for late spring and early summer in order to sustain downstream water demands. The increasing winter flood caused by rain-on-snow events could be important for water

resources management sectors and dam operation perspectives to sustain the downstream water demand further for ecosystem management and human consumptions in the low flow spring period.

1.1.2 Rain on Snow

The various precipitation forms (rain, snow and mixed) are observed across the cold and high-latitude region especially in cold seasons. Rain-on-snow (ROS) event has been defined in various ways in different studies, here the broad definition by Pomeroy, Fang, & Marks (2016) is followed; an event when rain falls on a snowpack. This study is focused on the total events rather than the extreme events of the ROS. The ROS is not a usual phenomenon, observed as an infrequent event in cold region Environment (Cohen, Ye, & Jones, 2015), but it is an important contributor to snowmelt induced flooding events (Pomeroy et al., 2016) in many cases because of its potential capacity to get melted the existing snowpack on the ground and creates an enhanced floods from rain and associated rain-induced snowmelt to downstream. The ROS has a complex generation process depending on air temperature, precipitation as rainfall and accumulated snowpack on the ground (McCabe, Hay, & Clark, 2007a). The ROS events are observed in maritime Mountain snowpack including US Pacific Northwest and Western Canada (Putkonen & Roe, 2003; McCabe, Hay, & Clark, 2007b; Mazurkiewicz, Callery, & McDonnell, 2008; Wayand, Clark, & Lundquist, 2017) and also recorded in eastern North America (Pradhanang et al., 2013a), central Europe (Garvelmann, Pohl, & Weiler, 2015), northern Eurasia (Ye, Yang, & Robinson, 2008) and Himalayas (Singh et al., 1997). The increasing frequency of the ROS events has been observed over the Canadian Prairies in recent years (Dumanski, Pomeroy, & Westbrook, 2015), as well as Rockies and West regions (Pomeroy et al., 2016) reporting massive flooding events to downstream. These regions have been receiving the increasing rainfall events even in the cold months (Shrestha et al., 2012), the recent trend of increasing ROS frequency could be enhanced by the precipitation phase change from snow to rain in the recent period in the response of atmospheric warming. The increasing trend of rainfall occurring in the winter snowpack can cause rapid melt and create a massive flood to downstream driven by rain-induced snowmelt than rainfall happens in the snow-free area. In western Canada, millions of people use river and river reservoirs for transportation and store snow-melt water in a reservoir for various purposes related to economic and ecological importance (Sturm, Goldstein, & Parr, 2018). The increasing ROS event could subsequently impact streamflow affecting the

peak timing, minimum flow of the cold months etc. The hydrological regime in this regional watershed is expected to go through the change or shift in future as seen the context that most of the mountain water regime in North America are likely affected by climate change associated ROS-induced flood events (McCabe et al., 2007b; Musselman et al., 2018) such as high flow in winter season, and subsequently low flow in spring seasons. The ROS can augment the flood risk due to additional runoff from snowmelt as compared to the equivalent rainfall event on snow-free land (Musselman et al., 2018). On ROS event, there is negligible or zero proportion of groundwater percolation as the surface and sub-surface is frozen condition and ground vegetation is almost in inactive condition. It allows all rains falls on the snow to convert into runoff and additional rain-induced snowmelt water cumulatively enhanced flood volume.

The ROS event is an important hydro-meteorological phenomenon which enhances the winter flooding in the cold region environment (Jeong & Sushama, 2017b), more importantly in flood forecasting and risk management sectors (McCabe et al., 2007a; Pradhanang et al., 2013b; Surfleet & Tullos, 2013)). The increasing frequency of ROS events could potentially cause serious physical and ecological damages such as downstream flood and physical damages etc. A devastating flooding and physical damages have been reported in the ROS event happen in the Canadian Rockies in June 2013 (Pomeroy et al., 2016) . Similarly, series of various ROS impacts have been documented for Eastern and Western region of North America where ROS-induced winter flood has been reported frequently (Graybeal & Leathers, 2006) and Feb 2017 near failure of Oroville dam with physical damages and evacuation of 190,000 people (Musselman et al., 2018). Another example of ROS flooding was 11.5 cm rainfall fell on 115 cm snowpack of the Catskill Mountain region melted rapidly causing historically massive floods throughout the region in Eastern North during 18-19 January, 1996 (Pradhanang et al., 2013). Importantly, the ROS event in the Catskill Mountains melted around 10 times more snowpack generating recorded winter flood than the same amount of rainfall could generate in the snow-free condition in 2 days which was historically high volume and rapid melt of such a big pile-up snowpack. The ROS plays a significant role in generating high stream flow and extreme floods more than it does radiation-induced snowmelt process (Huntington, Hodgkins, Keim, & Dudley, 2004; Jeong & Sushama, 2017a). The impact of ROS event to downstream areas depends on the intensity of rainfall on snowpack, snowpack depth and extent, snow water equivalent (SWE) and air temperature etc. The ROS events accelerate the snowmelt processes and increase the ROS-

induced runoff more than the radiation-induced snowmelt in the spring period. The study of ROS distributions and frequencies drills down to explore how the hydrologic regime is being changed in response to the ROS events such as winter flooding, snowmelt time-shifting earlier from the early spring to mid to late winter period with associated landslides and soil erosions and eventually changes channel morphology and entire hydrological cycle (Pradhanang et al., 2013).

It is expected that climate change potentially changes the ROS distribution and frequency in the future, with likely implications for flood risk and water resource management. The projection of the ROS changes over North America using regional climate models indicates an increasing trend towards northern latitudes (>50˚N) associated with increased rainfall and decreasing at low latitude (<50 ℃N) because of declining snow-covered days on the earth surface (Jeong & Sushama, 2017b). Air temperature has a major contribution to control over the ROS event frequency. In general, the air temperature proximate toward 0℃ while snow on the ground enhances the frequency of the ROS events. As the air temperature is proximate to 0℃, the subsequent precipitation phase is expected to change from snow to rain while falling to the earth surface and increase the rainfall event on the frozen surface and eventually the ROS frequency is expected to increase. When the temperature exceeds the freezing level for a longer period, the temperature is not favorable to retain snowpack on the ground and subsequently decreasing or negative ROS is expected in the future (McCabe et al., 2007b). Even though, the ROS is infrequent, only occurs a few times throughout a year, the ROS event has a visible impact on the hydrological cycle to generate high stream flows with the potential risk of generating floods than does radiation-induced snowmelt s(Cohen et al., 2015), for example the ROS-induced flood in the Catskill Mountain region during 18-19 January 1996 (Pradhanang et al., 2013). It is important to analyze the ROS trend to understand the potential evolution in the future. The projection of future ROS change on the regional scale is another avenue to understand how the evolution of ROS can affect the cold region hydrologic regime in the future. Most of the previous ROS studies are focused on station based observational data which are not sufficient to assess the spatial distribution of ROS and its response with different elevation levels. Recently, few recent studies have presented the spatial distribution of ROS and analyzed the ROS frequency in different elevation levels. Jeong & Sushama (2017) presented the spatial distribution and frequency of ROS in different elevation bands which demonstrate an elevational and spatial responses to the ROS distribution. In general, decreasing ROS days was observed in

response of the increasing temperature and decreasing snow cover days in low elevation while increasing ROS frequency in high elevation of Western region of US between 1969-2003 period (McCabe et al., 2007a). Similarly, a positive correlation of ROS days with elevation has been reported from the North-Eastern region of United States (Pradhanang et al., 2013) which demonstrates the elevation factor as another dimension of the ROS evolution in cold environment. The GSFLOW hydrological simulation used for future extreme event evaluations, driven by downscaled GCMs for the SRES A1B and B1 scenarios, also observed decreasing trend of the ROS-induced runoff in the low elevation zones and increasing trend in the high elevation zone of mountainous river basin, Oregon, US (Surfleet & Tullos, 2013). These recent studies in the North American mountainous regions strongly suggest that the precipitation and snowpack distribution in different elevation ranges have different response to ROS evolution (Surfleet & Tullos, 2013; Jeong & Sushama, 2017).

1.1.3 Study Area and climatology

The Fraser River Basin (FRB) in the province of British Columbia, Canada, is one of the largest watersheds in North America, draining to the western Cordillera (Benke and Cushing, 2005), extending from Pacific coast to the continental interior over 240,000 km^2 comprising the major tributaries of FRB are the Nechako, Quesnel, Chilcotin, and Thompson Rivers within the Interior Plateau (Islam, Déry, & Werner, 2017). Its elevation ranges from sea level to 3954 m at its tallest peak, Mt. Robson in the Rocky Mountains region (Benke and Cushing, 2005). The Fraser river's headwater is in the Rocky Mountains and runs through interior plateau towards the Southwest coast with a length of about 1400 km before discharging into the Strait Georgia (Schnorbus, Werner, & Bennett, 2010). The FRB has a variety of geomorphological features with 12 ecoregions and 9 biogeoclimatic zones and the land cover dominated by Coniferous forest (around 75%), followed by the alpine environment (17%) and various non-forest vegetation (8%) (M. Schnorbus et al., 2010). Around 63% of BC's population resides in FRB with a larger economic and social hub in BC. As the river emerges onto lower Fraser Valley, it passes through a series of dams for agricultural water supply and water regulations (Rice, Church, Wooldridge, & Hickin, 2009). The floodplains and delta areas exhibit a mix of agricultural, residential and commercial land and the streams and lakes water in FRB watershed provides the spawning habitat for eastern Pacific salmon breeding (M. Schnorbus et al., 2010).

The major water consumptions are agricultural and municipal supply, dams and reservoirs (Gray & Tuominen, 1999).

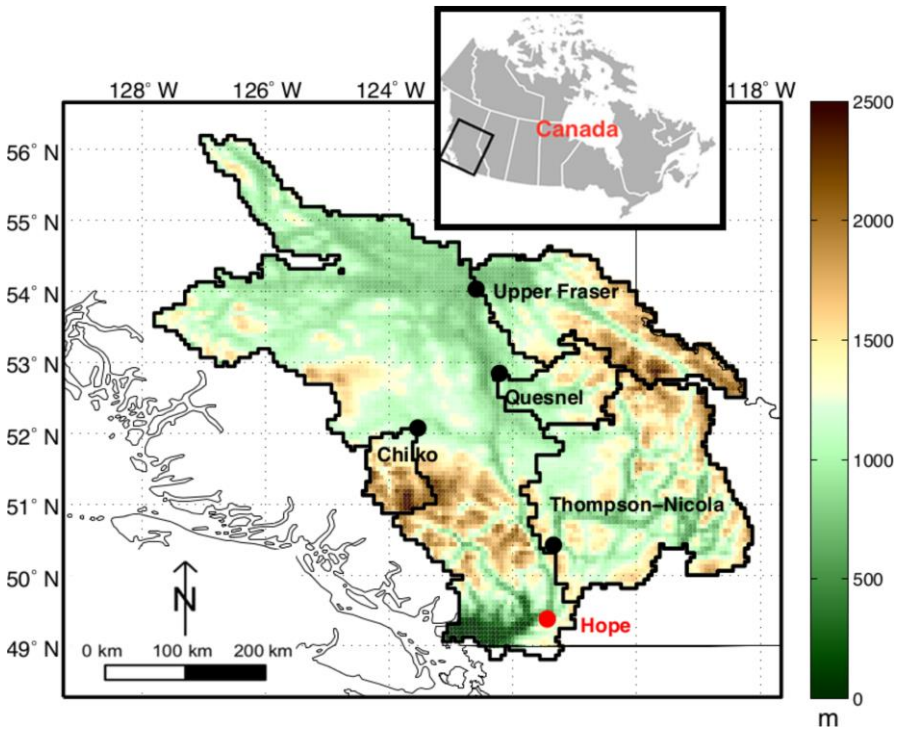

Source: (Curry & Zwiers, 2018)

Figure 1: Digital elevation map of the FRB with major sub-basins: Quesnel (QU), Chilko (CH), Thompson–Nicola (TN), Upper Fraser with a major outlet for FRB at Hope with a red dot.

As the FRB exhibits different biogeoclimatic zones, the mean annual temperature and precipitation vary spatially. The spatial variability of the mean annual temperature is between -1℃ to 6℃ and annual precipitation is between 200 to 2200 mm based on observed data from Natural Resources Canada (CANGRID) (figure 2). The mean annual surface air temperature in the FRB has been risen by 1.4℃ in the past 60 years affecting the natural water cycle in FRB (Kang, Shi, Gao, & Déry, 2014) and the trend would be higher in future with high vulnerability on the water cycle. The FRB generally receive higher precipitation in eastern and western mountain ranges compared to the inner landmass region and exceptionally extreme high precipitation in low laying outlet region due to the local orographic precipitation phenomenon of land-ocean interaction created by the proximity to the Pacific Ocean (Shrestha et al., 2012). The FRB exhibits different hydrologic response in different sub-regions varying snow-dominant, hybrid (rain and snow) and rain dominant at the different part of the basin (Wade, Martin, &

Whitfield, 2001; Shrestha et al., 2012; Siraj Ul Islam & Déry, 2017), with snowmelt induced flows occurs especially in late spring and early summer in current climatic condition (Islam & Déry, 2017). As the temperature has risen in the historical period, reduction of snow accumulation duration is expected to contribute earlier shifting of snowmelt-driven runoff and subsequently reducing summer flows (Kang, Gao, Shi, Islam, & Déry, 2016).

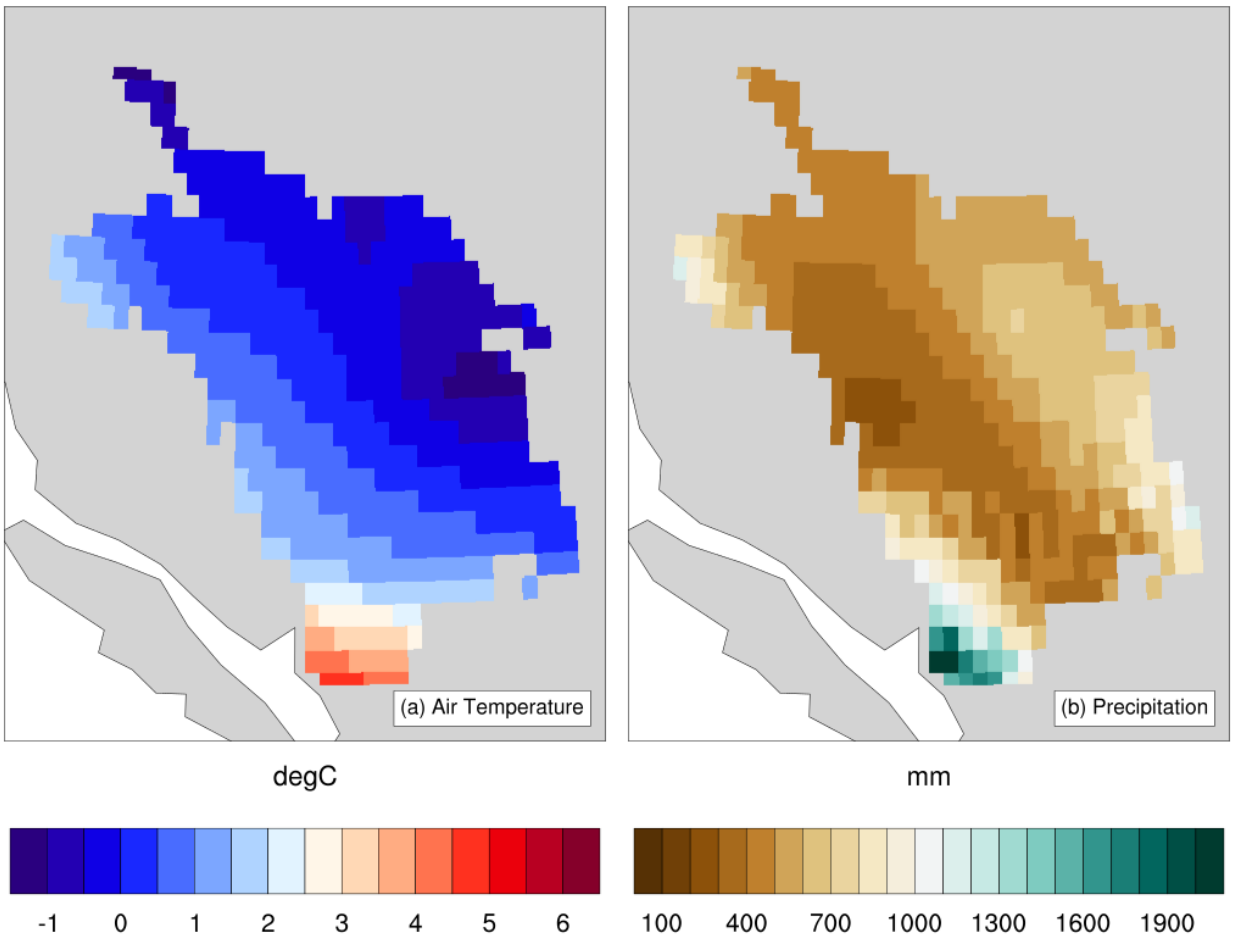

Data Source: (Hutchinson et al., 2009)

Figure 2: Spatial variability of the 30-year (1981–2010) mean annual temperature (℃) in panel (a) and mean annual precipitation (mm/year) in panel (b) for the Fraser River Basin based on CANGRID data from Natural Resources Canada.

Several winter rainfall and associated snowmelt flooding events have been reported in Fraser Valley. Recently on 18 December 2018, heavy winter hit of rain hammer on heavy snow was reported with the associated flood to downstream ("Winter wallop: Heavy snow, rain hammer southern B.C., CTV News," 2018). Additionally, CKPGToday reported research highlights

conducted form UNBC that future winter flooding is expected with shorter winter and increasing rainfall ("UNBC study warns of future flooding in Fraser River basin," 2019). The increasing rainfall can accelerate snowmelt in the high elevation region's snowpack and creates rain on snow induced floods in the future.

1.2 Aims and Objectives

The main goal of this research is to examine the projected changes in ROS events in long-term future (up to 2100) in the Fraser River Basin area using high-resolution climate and hydrologic modeling data to address the following objectives:

a) What changes can be expected in the short-medium- long-term (up to 2100) frequency of ROS events in the FRB in the response of climate change?
b) What are the primary physical drivers of the changes?
c) What is the response of ROS-induced surface runoff in the future?

1.3 Thesis structure

The remaining chapters of this thesis are structured as follows. Chapter 2 presents details about the data and methodology used in this research, including a brief background on the hydrologic model, and metric used to quantify Rain-on-Snow events. Chapter 3 presents the results including evaluation of annual and seasonal climate, and an examination of ROS events for historical and future scenario periods. It also discusses the responses to climate change of ROS events stratified by elevation, as well as the ROS-induced runoff changes. Chapter 4 presents a discussion of the results, a summary of the physical drivers of the future changes in ROS, and ROS-induced runoff. Finally, Chapter 5 summarizes the overall conclusions of this study.

Chapter 2: Data and Methodology

2.1 Model Simulations

a) Variable Infiltration Capacity (VIC) model Description

The Variable Infiltration Capacity (VIC) model is a semi-distributed macro-scale hydrologic model developed by Liang et al. (1996) which has been extensively used in studies related to water resources management, land-atmosphere interaction and climate change (Wen, Liang, & Yang, 2012; M. Schnorbus et al., 2014; Siraj U Islam et al., 2017)). The VIC model also provides a land surface scheme when coupled to a general circulation model, it balances both the water and surface energy budgets within the grid cell and sub-grid variations are captured statistically (Liang, Lettenmaier, Wood, & Burges, 1994; Liang et al., 1996).

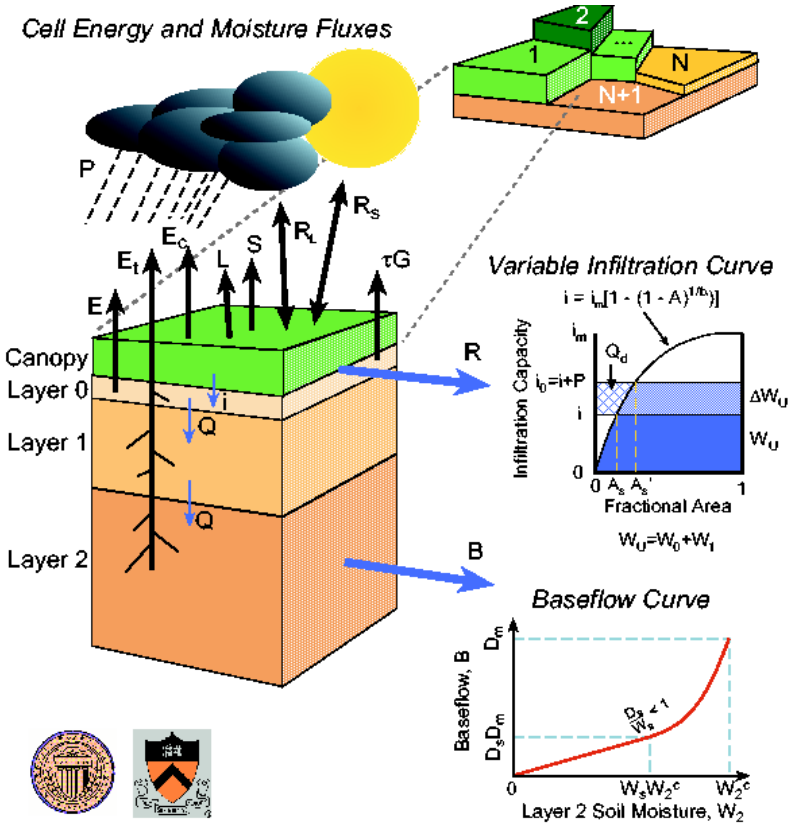

(Gao et al., 2010)

Figure 3: Schematic of the VIC model with the mosaic representation of vegetation coverage.

Over the years, a series of modifications and improvements have been made in VIC to improve the model's capacity dealing with the complex hydrologic process. The grid-based VIC represents the vegetation heterogeneity, variable infiltration and non-linear base flow (Gao et al., 2010). The overall VIC model framework has been described in detail in literature (Liang et al., 1996; Nijssen, Lettenmaier, Liang, Wetzel, & Wood, 1997) and the major characteristics of the VIC can be pinpointed as follows; the representation of vegetation heterogeneity, non-linear base flow and variable infiltration into multiple soil layers (as shown in figure 3).

The VIC model can be run in two different modes: a water balance mode, and a water and energy balance mode (Liang et al., 1996). The full water and energy balance mode solves water balance and computes the surface energy balance to determine the fluxes (sensible heat flux, ground heat, ground heat storage, outgoing longwave radiation and indirect latent heat) to calculate the snowpack accumulation and ablation process in spatial scale (Gao et al., 2010). The water and energy mode of the VIC model computes the output of snowfall, rainfall and SWE from the input of precipitation in response to critical temperature in the prescribed environment (such as land use) in the digital elevation model (DEM).

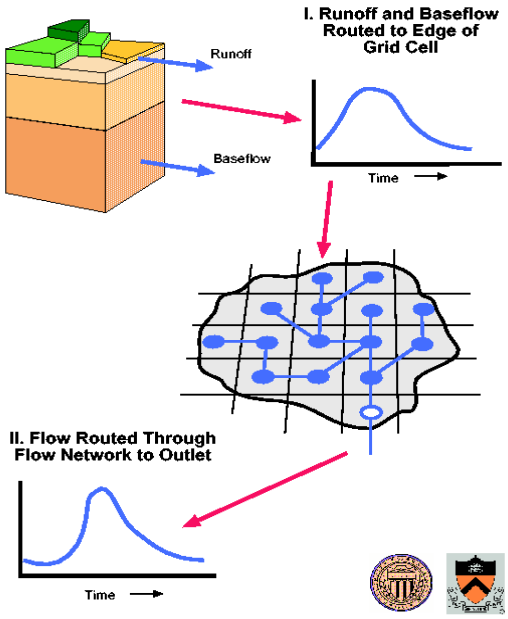

(Gao et al., 2010)

Figure 4: Schematic of VIC network routing models.

Additionally, the VIC model calculates runoff in each grid cell for a daily time series. The VIC computes runoff for each grid cell and unidirectional transforming to the low laying surrounding grid cell (Figure 4) (Gao et al., 2010). The additional extension of the routing model is employed to transport the surface runoff and baseflow to the outlet of each grid cell and eventually into the river system without allowing flow back from the channel to grid cells (Gao et al., 2010; Rodell et al., 2004; Liang et al., 1996). River routing module can be implied to compute the collective runoff throughout the basin into the river channel. (Gao et al., 2010). Once the runoff is channeled out to the subsequent grid, it is counted as no longer part of the water budget of these grid cells. Here, only spatial gridded runoff (total runoff and the ROS-induced runoff) has been considered to explore the spatial variability. The river routing module of the VIC model will not be discussed, and the channeled runoff will not be used in this study. The purpose of using spatial runoff is to correlate the spatial ROS events and spatial ROS-induced runoff.

b) Boundary Conditions

The VIC hydrologic model's simulation output, driven by atmospheric forcing of 21 different Global Climate Models (GCMs) (see in table no. 1 in appendix) that participated in the Coupled Models Intercomparison Project Phase 5 (CMIP5) are used for the analysis of ROS event and the ROS-induced runoff in the Fraser River Watershed. The historical and RCP8.5 simulations from CMIP5 were employed in this study for historical and projected ROS analysis. In the RCP 8.5 scenario, the historical greenhouse gas and aerosol forcing are imposed up to 2005, and after that the external forcing follows Representative Concentration Pathway 8.5 (Taylor, Stouffer, & Meehl, 2012). In this analysis, two different time periods are used; the Historical period from 1970 – 1999 to compare with the observed trend while the scenario period from 2070 – 2099 is used to project the future changes. Additionally, multidecadal and seasonal (winter (DJF), spring (MAM), summer (JJA) and Fall (SON)) ROS distribution has been projected from the near future (2020-2039) to long term future (2080-2099).

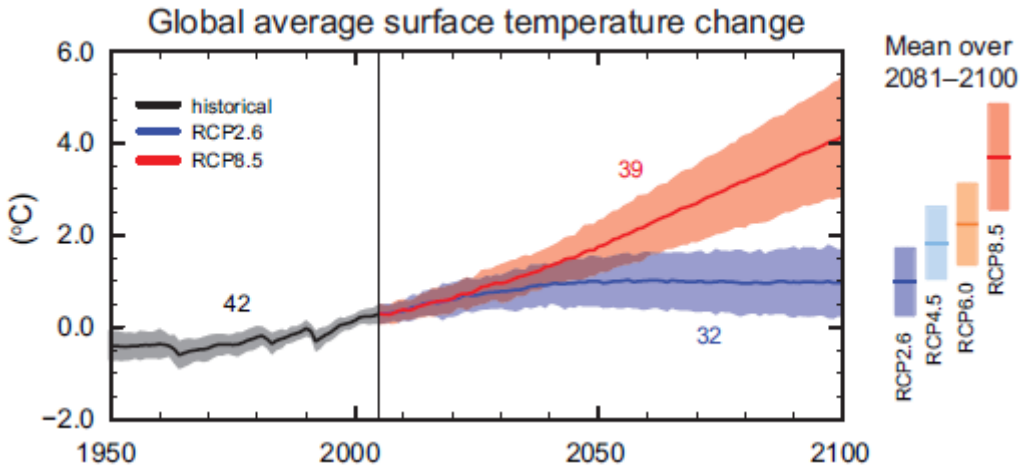

Source : (IPCC, 2013, p. 23)

Figure 5: CMIP5 multi-model simulated time series from 1950 to 2100 for change in global annual mean surface temperature relative to 1986-2005. The time series of the projections and a measure of uncertainty (shading) are shown for scenarios RCP2.6 (blue) and RCP 8.5 (red) and the black (gray shading) is the modelled historical evolution using historical reconstructed forcing (observed GHG, aerosol forcing and natural climate forcing).

The RCP is defined as the radiative energy trapped per unit square meter area on the earth's surface. The different trajectories of RCPs are used based on emission scenarios, such as RCP 2.6, RCP 4.5, RCP 6.0 and RCP 8.5. The RCP 2.6 w/m^2 is the improved and less Green House Gas (GHG) emission scenario while RCP 8.5 w/m^2 is the business as a usual scenario which means the highest GHG emission trend (IPCC, 2013, 2014). Historically GCMs simulate earth climate driven by GHG emission and aerosol forcing to capture the observed trend (Figure 5). In the long-term future, future emission scenarios and internal variability of the earth system are uncertain which increases the inter-model variability.

2.2 Data Sources

The observed ROS event is calculated using CANGRID rainfall (Hutchinson et al., 2009) and blended-4 SWE (Mudryk, Derksen, Kushner, & Brown, 2015) dataset to compare with historical ROS for the period of 1970-1999. The CANGRID precipitation is a set of Canadian gridded observed precipitation data that was interpolated from the stations' data. The CANGRID interpolated precipitation demonstrates a smooth spatial pattern with slightly varies in sub-regional scale such as low precipitation in interior landmass and high in mountainous regions. The blended-4 SWE is a blended product of 5 different SWE datasets (Mudryk et al., 2015) with the aim to robustly characterize the spatial and temporal SWE climatology at the north

hemispheric level. The five different components of the Blended -4 SWE are 1) the satellite-based product, the GlobSnow, version 2 (http://www.globsnow.info/) (Takala et al., 2011); 2) the Global Land Data Assimilation System (GLDAS), version 2 (https://ldas.gsfc.nasa.gov/gldas) (Rodell et al., 2004); 3) the European Center for Medium-Range Forecasts interim land surface reanalysis (ERA-Interim/Land) (https://www.ecmwf.int/en/forecasts/datasets/reanalysis-datasets/era-interim-land) (Balsamo et al., 2015); 4) the Modern-Era Retrospective Analysis for Research and Applications (MERRA) (https://gmao.gsfc.nasa.gov/reanalysis/MERRA/) (Rienecker et al., 2011); 5) Crocus snow scheme SWE product (Brun et al., 2012). The observational ROS is compared with the historical ROS trend in the period of 1970 - 1999. The high resolution (0.06° x 0.06°) precipitation data from CANGRID is upscaled to the resolution of the blended 4 SWE product (1° x 1°) and filter only rainfall days using the temperature threshold which is mentioned below (in section 2.3), and both the CANGRID rainfall and the blended-4 SWE are used to compute the observed ROS trend for 1970 - 1999. The overall study period is split into historical (1970-1999) and scenario (2070-2099) periods and additionally we consider the future projection period into near term-future (2020-2039), medium-term future (2040-2059) and long-term future (2060-79) in this study to analyze the multidecadal change trend for long term projection. The CMIP5 input was downscaled to 0.25˚x0.25˚, and bias corrected using the Contracted Analogue Quantile Mapping Method, version 2.0 (Islam, Déry, & Werner, 2017; Islam, Curry, Déry, & Zwiers, 2018). The bias corrected data was used to evaluate the VIC hydrologic model for historical and scenario period up to the end 21st century (Siraj Ul Islam et al., 2018). The CMIP5 driven VIC hydrologic model output data (rainfall, SWE, runoff) and CMIP5 input data (temperature) from Islam, Curry, Déry, & Zwiers (2018) are used in this study for the projection of the ROS events, describing physical mechanisms, and the ROS-induced runoff changes in future.

2.3 Quantifying rain-on-snow events

The variables used for the ROS study are spatially-resolved rainfall, SWE, and runoff from the VIC simulation in historical and scenario period. As the basin area has diverse physiographic and hydroclimatic conditions (Siraj Ul Islam et al., 2018), the best approach to deal with the diverse variability is the elevational zonation of the river basin and analyze the climate response to the ROS in different elevational zones. The entire basin area (0 to 3954 m elevation) is divided into four different elevation bands, i.e. 0 – 500 m, 501 – 1000 m, 1001-1500 m and 1501 m &

above. The idea of partitioning the watershed into the four elevation zones is developed after evaluating the temperature and precipitation trend across elevation: significant change of temperature and precipitation was detected around the elevation of 500 m and 1000 m (figure not shown) and the elevation range above 1501 m is kept in a single threshold zone because there is only some high mountain peaks beyond 2000m. even though the elevation band <500 m has least number of sample size i.e. 17 grid boxes, it is separated as a single elevation band as rapid warming trend is observed over there. Most of the area of the lowest elevation band (0 – 500) m lies close to the ocean and surrounding by the Coast mountains where the annual climate is relatively warm and wet in the response of local orographic phenomenon. The 0 – 500 m region of the basin outlet is excluded in most of the analysis below as this low laying area receives extremely high rainfall and warm annually (figure 2) (the extreme high precipitation and temperature at the outlet section compared to overall basin area). The highest elevation band (1501 m and above) has a larger threshold range but most of the area falls under this band is below 2000 m and only a few highest peaks of mountains have the highest elevation.

a) Classification of ROS Days

Rain-on-snow (ROS) events occur when liquid precipitation (rain) falls onto a surface covered by a snowpack. To obtain liquid precipitation at the surface requires both the occurrence of precipitation, and near-surface air temperatures (T_{as}) above freezing. To quantify ROS events, therefore, requires data on total precipitation (mm), rainfall (mm), snow water equivalent (mm SWE), T_{as} (˚C), and surface runoff (mm). In this study, we extracted these variables on the spatial grid from VIC simulations, and from observational sources, at daily mean frequency. As the VIC simulation and observational data have daily time series data, we prefer to use the daily data because the daily average is much clear to compare with future changes.

We apply the same partitioning procedure implied in VIC simulation to the observed data. In the VIC simulation, total precipitation is categorized as 100% rainfall for temperature above 1.5˚ C, 100% snowfall for temperature below 0.5℃ and mixed type for the temperature between these two thresholds (Siraj Ul Islam et al., 2018). The first step is to partition the daily total precipitation into the snow, rain and mixed types. This allows us to separate out the amount of rain falling onto the snow. All precipitation recorded while daily mean T_{as} < -0.5 ˚C is counted as snow, precipitation that occurs while daily mean T_{as} > 1.5˚C is counted as rain, and precipitation recorded when the daily mean T_{as} is between -0.5˚C to 1.5˚C is counted as mixed precipitation.

For temperatures in this range, the fraction of mixed precipitation that falls as rain (f_{rain}) estimated as a linear function of T_{as}: $f_{rain} = T_{as}/(1.5\text{-}0.5)$, and the fraction of snow is $f_{snow} = 1 - f_{rain}$. The values f_{rain} and f_{snow} are multiplied by the daily total precipitation to yield rain and snow accumulation amounts for those days.

We define a rain-on-snow (ROS) event to have occurred at a particular grid cell, in a given day, when the following joint conditions are met:

Total daily rainfall > 0.5 mm and SWE > 0.5 mm.

The ROS events were counted for each grid cell separately, before any spatial aggregations were applied. Note that because the available model output is for daily averages, a maximum of one ROS event can be defined per day. The threshold of 0.5 mm for rain and SWE used to filter ROS events was selected because it relates to the environmental lapse rate, surface air temperature is relatively lower in high elevation regions with higher snow thickness and extent compared to low elevation favoring longer snow resident time on the ground. The spatial map clearly showed the low, medium and high elevation regions have relatively shorter, medium and longer snow resident time respectively. Below 500 m, we detected the aggressive changes in precipitation, temperature and SWE which motivated to split the basin area in the interval of 500 m elevation to evaluate the altitudinal responses to the ROS. Jeong & Sushama (2017) analyzed the basin-scale ROS with the response of Elevation which showed a continuous increase of the ROS events as moving to high elevation zones. The US navy topographic data (https://www.ngdc.noaa.gov/mgg/global/etopo5.HTML) was first masked by the FRB area and then split into four different elevation mask files. The elevation mask files were applied to all variables before computing averages, to isolate the impact of elevation.

Chapter 3: Results

The observational precipitation, temperature and ROS event trend is examined seasonally over the FRB. Additionally, the future temperature, total precipitation, rainfall changes and the associated future ROS evolution is analyzed. The spatial distribution of historical and future changes of ROS in annual and seasonal scale are examined to explore seasonal variations, as well as corresponding seasonal and annual changes in the future. Furthermore, the rainfall, temperature and associated ROS in different elevation zones are examined to explore the potential drivers of future ROS evolutions in different elevation zones. The correlation analysis of the future changes of the ROS, rainfall, temperature and SWE with respect to elevation bands is examined for explicit analysis of the different controlling factors of the ROS change in the future. This is followed by the discussion of the ROS feedback to the ROS-induced surface runoff changes in different elevation zones to examine the ROS impact on surface runoff.

3.1 Seasonal Climate

3.1.1 Observed Rainfall Climatology

The seasonal rainfall greatly varies over the FRB. Winter season (December, January and February (DJF)) receives the lowest while the summer season (June, July, and August (JJA)) receives the highest amount of precipitation across the basin. There is heterogeneity pattern of precipitation distribution across the basin. The interior plateau (wider central region) and leeward side of the Coastal Mountains receive less than 200 mm of precipitation in a year compared to the Rocky Mountain region in the east which receives around 700 – 900 mm/year. In DJF, the rain shadow region receives the precipitation ranges from 0 to 25 mm while most of the areas receive 30 - 50 mm precipitation. In March, April and May (MAM), the eastern part of the river basin receives relatively more precipitation than in the western part of the basin. It has a clearly distinct precipitation pattern in the Coast and Rocky Mountains in MAM. The JJA receives predominantly higher precipitation across the basin ranges from 250 - 350 mm with predominantly high in Rocky Mountains region. In September, October and November (SON), there are several diagonal patches of precipitation patterns with the increasing trend towards the northeast. Most of the precipitation falls in Coast and the Rocky Mountains, predominantly as a snowfall. The south-western section of the basin (outlet to the Pacific Ocean) receives relatively higher precipitation in all seasons as compared with the entire basin area which is dominantly

governed by local phenomenon i.e. orographic precipitation. The low elevation southern outlet region receiving rain all around the year does not have any significant implication in the watershed scale as the runoff generated in the low elevation region quickly drains into the ocean. The extreme high rainfall in the outlet section is not being discussed and analyzed in detail as it does not impose any considerable impact on the watershed.

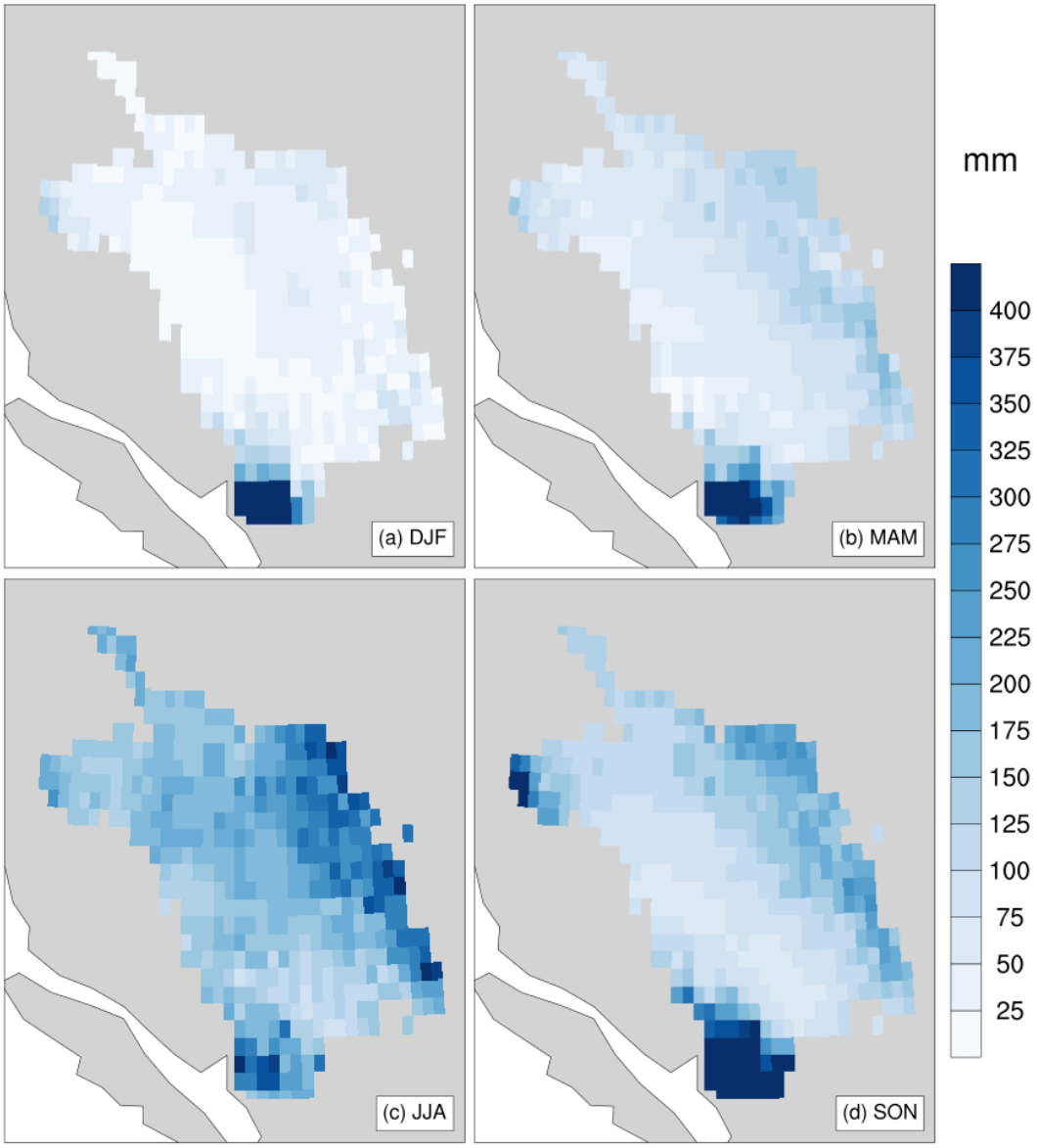

Figure 6: Observed Seasonal (Winter (DJF), Spring (MAM), Summer (JJA) and Fall (SON)) Precipitation of the Fraser River Basin for 1970 to 1999 based on CANGRID data from Natural Resources Canada

3.1.2 Observed Temperature Climatology

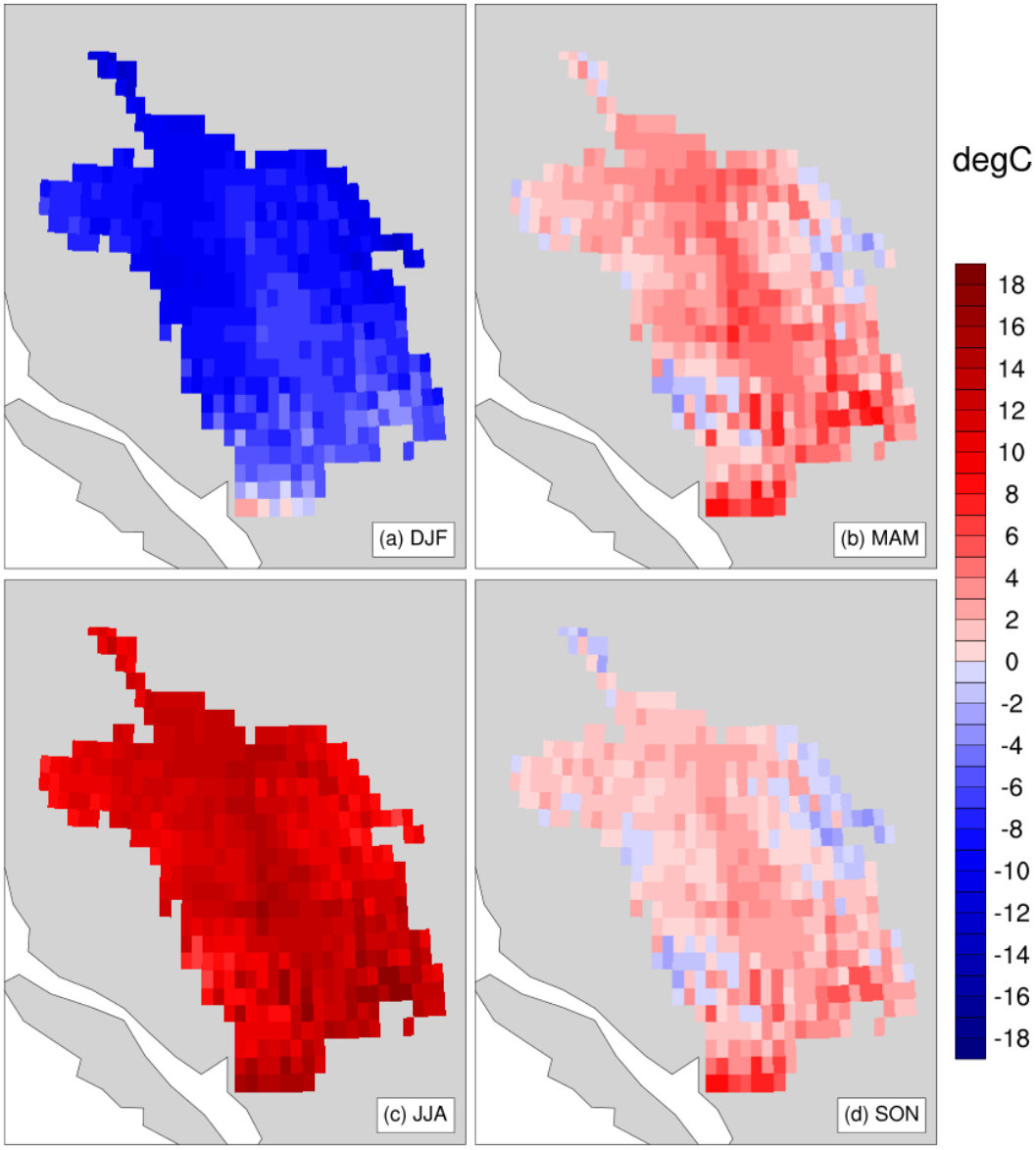

Figure 7: Observed Mean Seasonal (DJF, MAM, JJA, SON) Temperature of Fraser Basin for 1970 to 1999 based on CANGRID data from Natural Resources Canada

Similarly, the FRB exhibits a spatial variation of mean seasonal near-surface air temperature. Mean monthly temperature ranges from -2 to -10℃ in Winter (DJF) with the lowest mean temperature in mountain regions and the northern part of the river basin. The mean monthly temperature of MAM is range from 0 to 6℃ with relatively warmer interior plateau region and southern part of the basin and relatively low mean temperature in Coast and Rocky mountainous ranges. Similarly, the mean monthly temperature of JJA has the ranges from 6 to 14℃ which is relatively warmer in the interior region and southern part of the basin compared to east and west

mountain ranges. The entire watershed area has relatively warmer air temperature in summer which is obvious in the northern hemispheric region. The mean monthly temperature of SON drops down ranges from -2 to 4℃ from the warmest JJA season. In SON, the interior region and southern section have a relatively warm temperature i.e. close to 0℃ while the mountain ranges receive around -2℃ temperature.

3.2 Temperature and Precipitation Change

3.2.1 Temperature Change

The multi-model ensemble (MME) mean temperature in all seasons and elevation ranges is expected to increase in the future. In the lower elevation region (<500 m), the average winter temperature is close to the freezing point (or slightly above the freezing point at the coastal grid) and continuously increasing in the long-term future which will not favorable for snowpack accumulation for long term. Moving to higher elevation regions, the average winter temperature is critically important which is below the freezing level in the near-term future, but the winter temperature is continuously warming and proximate towards 0℃ in medium to long term future.

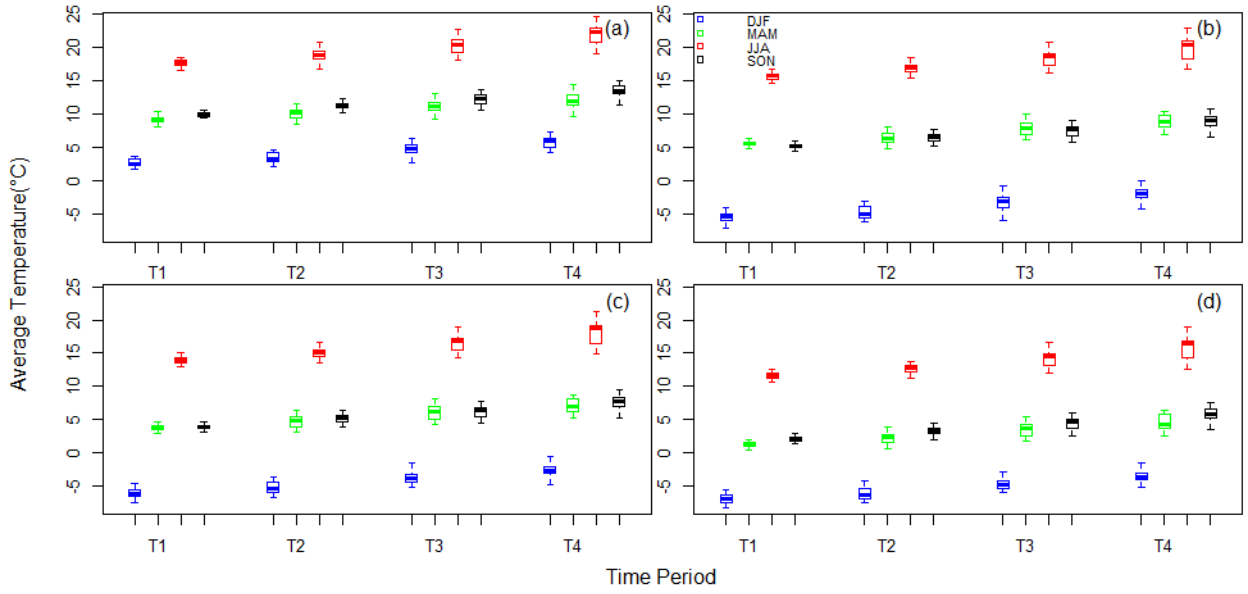

Figure 8: Average temperature distribution in Fraser River Basin presented in multidecadal (T1=2020-2039, T2=2040-2059, T3=2060-2079, and T4=2080-2099), seasonal (winter(DJF), spring (MAM), summer (JJA), and fall (SON)) in different elevation zones ((a)=0-500 m, (b)=501-1000 m, (c)=1001-1500 m and (d)=1500 & above m). Each boxplot length represents multi-model uncertainty and color indicates the season

As the temperature is proximate above the freezing line, the probability of precipitation as rain is likely to increase in the future. In elevation range 501 - 1000 m, the average winter temperature around -5℃ is continuously expected to increase in the long-term future towards 0℃. Similarly, higher elevation ranges (1001-1500 m and 1501 m & above) have average winter temperature -6℃ and -7℃ respectively and projections show a similar trend of warming in the long-term future. Other than DJF's seasonal average temperature is more than 0℃ even though the individual days could have a freezing temperature.

There is a clear trend of winter temperature in all elevation regions continuously increasing in the future with very small model uncertainties as compared to other seasons. Various types of uncertainties could be associated with the projected temperature such as internal variability, emission scenario and model uncertainty. Here the whiskers of the boxplots represent the model uncertainty, which for projected temperature is low in the near-term future, and gradually increases in the long-term future. The major governing factors of climate systems are highly uncertain to predict in a specific trajectory in the long-term future such as earth's internal variabilities, radiative forcing etc.

We further diagnose kernel density plot for the minimum temperature to estimate the probability density function (PDF) of the multi-model ensembled daily minimum temperature for Sept to May for historical and different projection periods to analyze the minimum temperature distribution shifting from the extreme cold to warm phase. The peak density distribution is monotonically shifting towards warmer range (proximate towards 0℃) from historical to long term future, additionally the minimum temperature density at or close to 0℃ is gradually increasing in the future which favors more likely rain events in future. The peak of the density plot is expected to shift from -12℃ to -5℃ from historical to projection period. As the high elevation region loss (shrinking and thinning) snowpack in the response of warming climate, snow albedo is expected to decrease, and the temperature increment would be more aggressive in high elevation. The minimum temperature is continuously shifting from near term future (2020-39) to long term future (2080-99) as seen in figure (9) below. As the minimum temperature is heating up more rapidly in cold seasons, it eventually response to precipitation for the phase change to likely occur more rainfall. The minimum temperature density distribution in the cold season in all projection periods indicates the increasing probability of the ROS in the future.

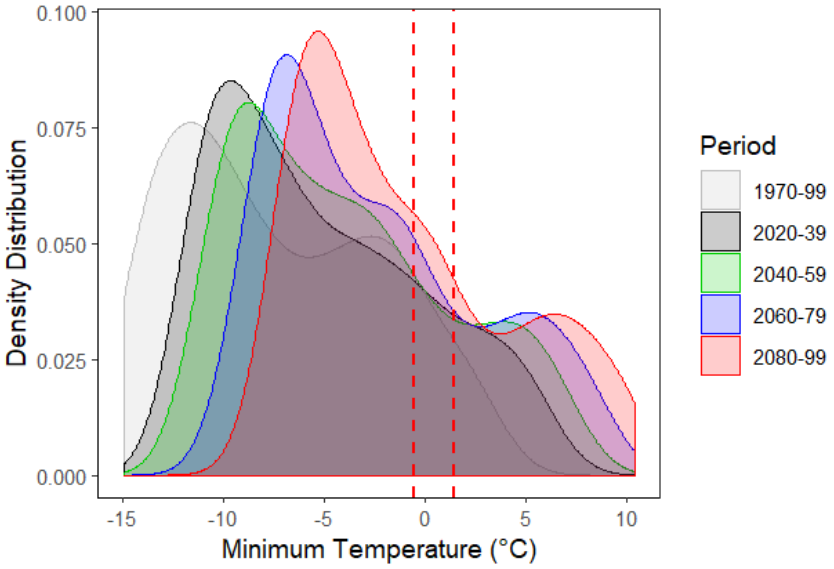

Figure 9: Minimum temperature density historical (1970-99) period for the different projection period (1970-99, 2020-39, 2040-59, 2060-79 and 2080-99) in FRB with the threshold to filter snow (<-0.5˚ c), rain (>1.5˚ C) and mixed type between these two thresholds.

3.2.2 Precipitation Change

Globally, projected changes in precipitation are positive with more intense and frequent events in the future with associated higher climate model uncertainties (IPCC, 2014). In general, the mid-to-high latitude of the northern hemisphere is expected to receive more precipitation in the future as Northern Hemisphere heats up faster than the Southern Hemisphere (Putnam & Broecker, 2017) which favors to increase evaporation process and hold more moisture in the atmosphere. The spatial average of MME mean precipitation rises continuously over the scenario period with closely 15% based on the historical period. The mid-latitude western Canadian region of extremely complex topography has a strong precipitation gradient (Erler & Peltier, 2016), expected to receive more precipitation in future climate dominantly in the winter season. As mentioned in the previous studies from (Islam, Déry, & Werner, 2017; Islam, Curry, Déry, & Zwiers, 2018; Kang, Gao, Shi, Islam, & Déry, 2016), the mean annual precipitation is expected to increase in the future period, the southwestern section of basin is expected to show a smaller increase (6 to 10 %) in total precipitation, while the northern and eastern sections of basin is expected to increase by double the amount (14 to 20% increases). 80% of GCMs members are agreeing to the sign of the projected change of total precipitation. The increase in precipitation is expected more dominant over the Rocky region while the Coast region receives slightly increment and the interior region receives the least increment.

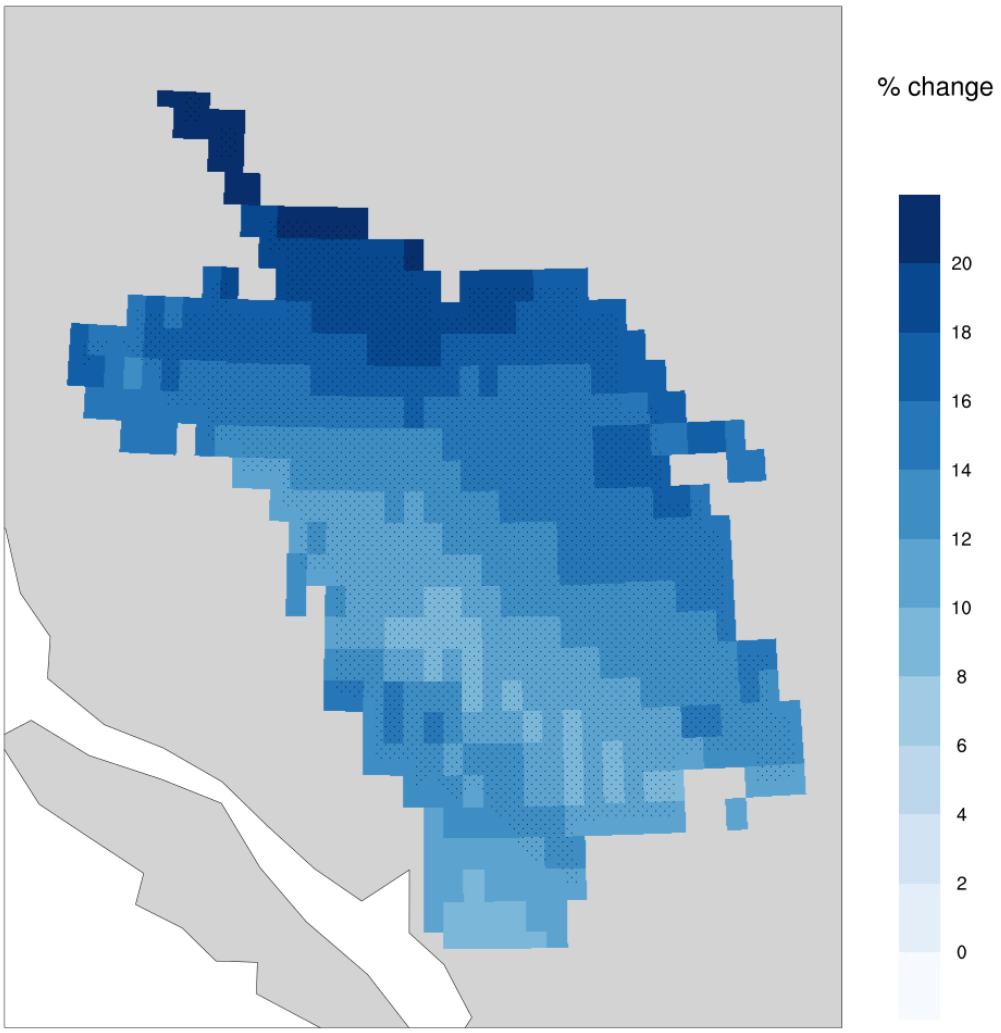

Figure 10: Climate change response to annual precipitation changes (scenario period: 2070-99 & historical period: 1970-99 in Fraser basin with the multi-model agreement (80%) to indicate the model agreeing on the change signal

The separating out of MME mean total precipitation into snowfall and rainfall shows different trends of rainfall and snowfall change up to the end of 21st century. The Coast Mountain region is expected to receive higher rainfall (80 to 100% increase) in the future which is driven by both the increase total precipitation and precipitation phase change from snow to rain in the future (Figure 11). The Rocky, Coast Mountains and the southern section of the basin are expected to receive the significant decreasing snowfall (60 to 90% decreases) and subsequently increasing rainfall with 90% of GCMs model agreeing to the sign of trend (Figure 11). In the Interior plateau region of the basin which receives less precipitation in general, it is

expected to decrease snowfall but a slight increase in rainfall in the future. The overall changes in total precipitation, rainfall and snowfall could have an impact on ROS frequency and distribution across the basin in the future.

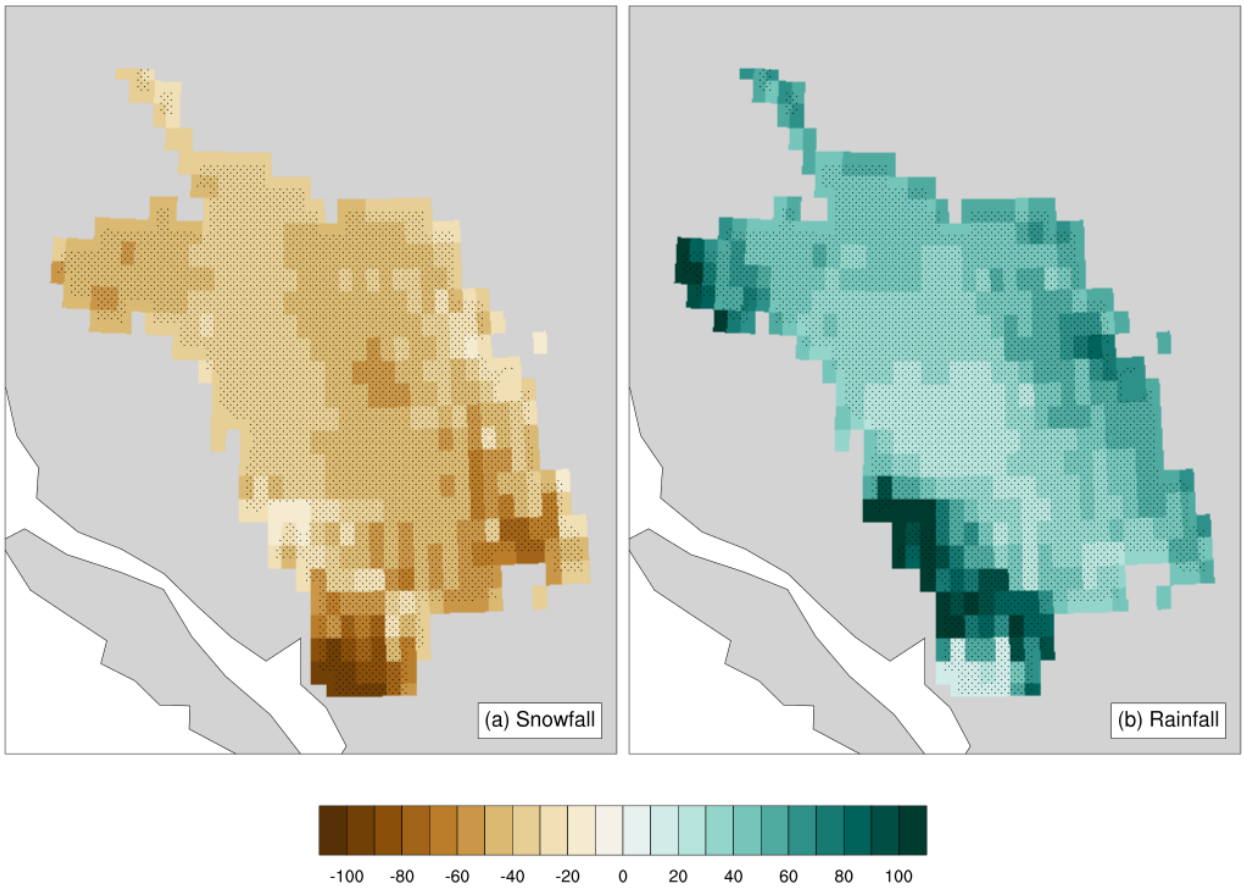

Figure 11: Precipitation phase changes in the future with the multi-model agreement (80%) to indicate the sign of future change

In the low elevation range, the total rainfall volume has a seasonal variation with high in winter and extremely low in the summer season. As the temperature is warm enough to exceed the freezing line in the low elevation range, the rainfall in the winter season does not associate with ROS events for long term future. As moving to higher elevation zones, all seasons except summer season are expected to receive continuously increasing rainfall in future and the winter rainfall is even more rapidly increasing with higher model uncertainties in long term future. The whiskers of the boxplot represent the model uncertainty, which for projected rainfall is relatively high in winter as compared with other seasons. As the governing factors of climate system are highly uncertain in the long term future such as earth's internal variabilities, radiative forcing etc, the rainfall projection for the long term future has higher model uncertainties. The increasing

trend of winter rainfall in other than lowest elevation range is important to generate the future ROS evolution in these particular elevation ranges. Both rainfall and average temperature are continuously increasing in these elevations range other than < 500 m.

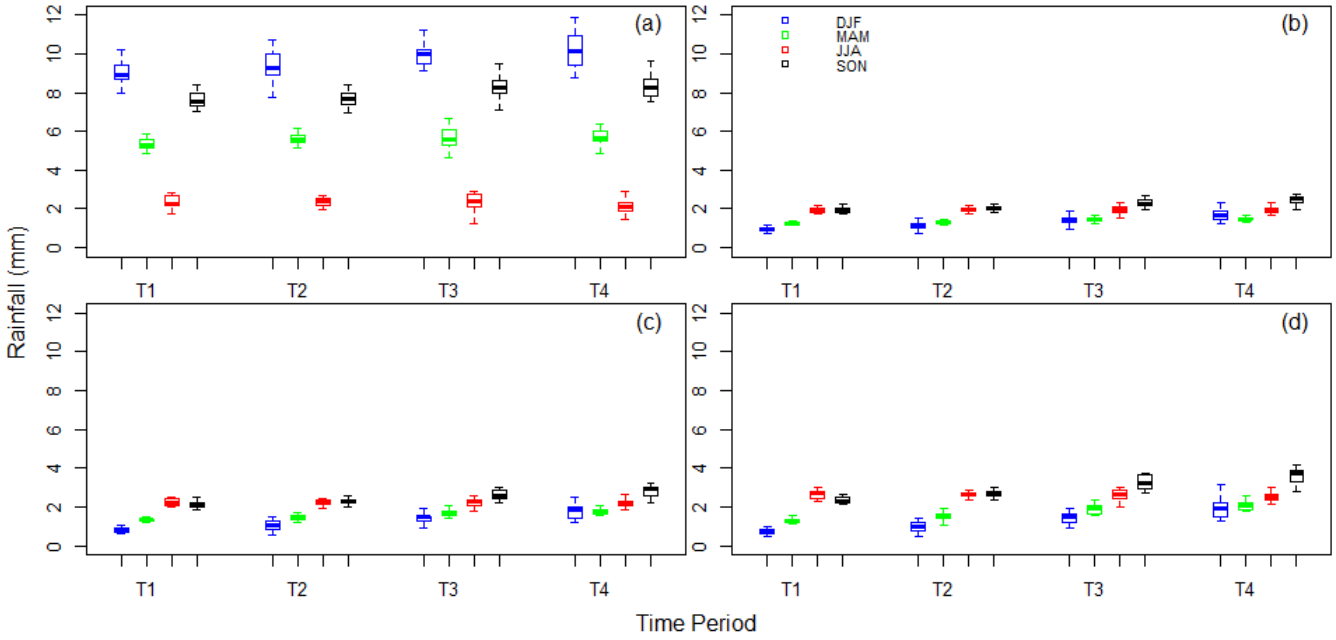

Figure 12: Rainfall distribution in Fraser Basin presented in multidecadal (T1=2020-2039, T2=2040-2059, T3=2060-2079, and T4=2080-2099) and seasonal (winter(DJF), spring (MAM), summer (JJA), and fall (SON) in different elevation zones ((a)=< 500 m, (b)=501-1000 m, (c)=1001-1500 m and (d)= > 1501 m). Each boxplot length represents multi-model uncertainty and color indicates the season.

3.3 Observed, Historical and Scenario ROS Events

The observed ROS distribution is examined across the FRB as shown in figure 13 panel (a) which seems relatively lower ROS day as compared to the historical plot in figure 13 panel (b), The observed spatial ROS distribution shows relatively higher in low elevation outlet section (60 days in a year) and west north part (50 days in a year) of the basin. Most of the basin area including the Rocky mountain has 10 -15 ROS days in a year while central par to the basin has relatively low ROS days (around 5 days in a year). The MME mean annual ROS distribution in the historical period and future ROS change is also examined across the FRB as shown in figure 13 (b) and (c). In the historical period, the high elevation regions of Coast and the Rocky Mountains receive 95 to 105 ROS days per year while low elevation areas of those two mountainous ranges received 60 to 65 ROS days per year. Compared to observed ROS days, the historical ROS days are more frequent even though the period of calculation is the same. Even

though the spatial variation trends seem similar in both the observed and the historical ROS events, the historical ROS frequency is dominantly high across the basin which clearly indicates there is bias either in one or both variables of the ROS counting i.e. rainfall and SWE. The bias associated with the model data does not have an influence on the end results of the future ROS changes because the bias in historical and scenario ROS is canceled out while computing the percentage changes of the ROS in the future. The trend of relatively high ROS in mountain regions and low ROS distribution in interior landmass is similar in both observed and historical plots in figure 13. The observed ROS shows the spatial trend such as higher ROS days in the west section, moderate ROS days in eastern and most of the basin areas and very few ROS days in the central and rain-shadow region. The larger portion of the river basin area i.e. interior plateau receives around 20 ROS days per year which is distinctly low as compared to the two mountain ranges in east and west part of the watershed. The spatial distribution of the ROS days follows the pattern of diverse physiographical and hydroclimatic conditions (as discussed in section 3.1), the larger range of annual ROS patterns has been observed in the FRB with high frequency in peak regions which has longer SWE resident period as compared to the low elevation ranges in interior landmass.

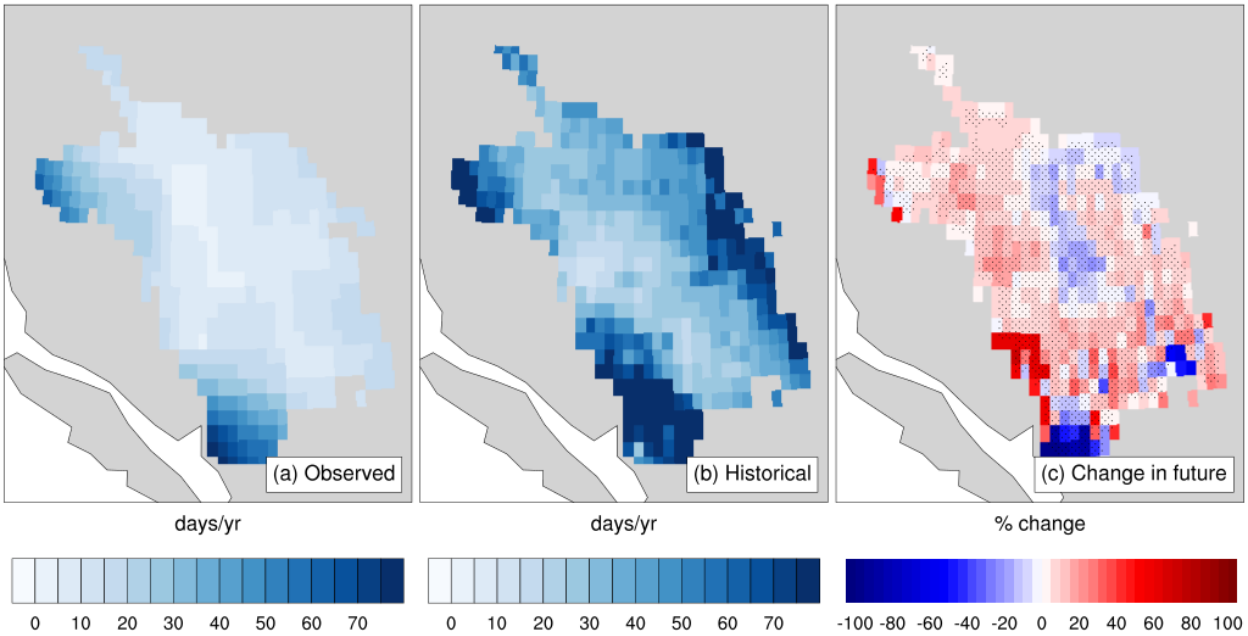

Figure 13: Annual ROS events of the observed (a), historical (b) and projected change in scenario (c). Panel (b) and (c) are MME with the multi-model agreement (80%) indicating the sign of future changes in panel (c)

The rain shadow region of Coast Mountains (western central part of the basin) receives only 15 ROS days in a year. The future change in ROS events in the basin area does not show any specific trend but most of the basin area is expected to receive increasing ROS frequency in the future by 15%. The high elevation area specifically mountain regions of Coast Mountain are expected to receive a high frequency of ROS events with 60% increment on average while some portion of the inner valley and outlet section of low land area are expected to receive slightly decreasing with -5% on average and rapidly decreasing with -100% ROS frequencies respectively. The ROS changes in the future are not linear with the historical distribution across the basin area. The MME mean ROS change indicates a different trend in different elevation ranges, such as inner valley, mountain ranges and peak of mountains.

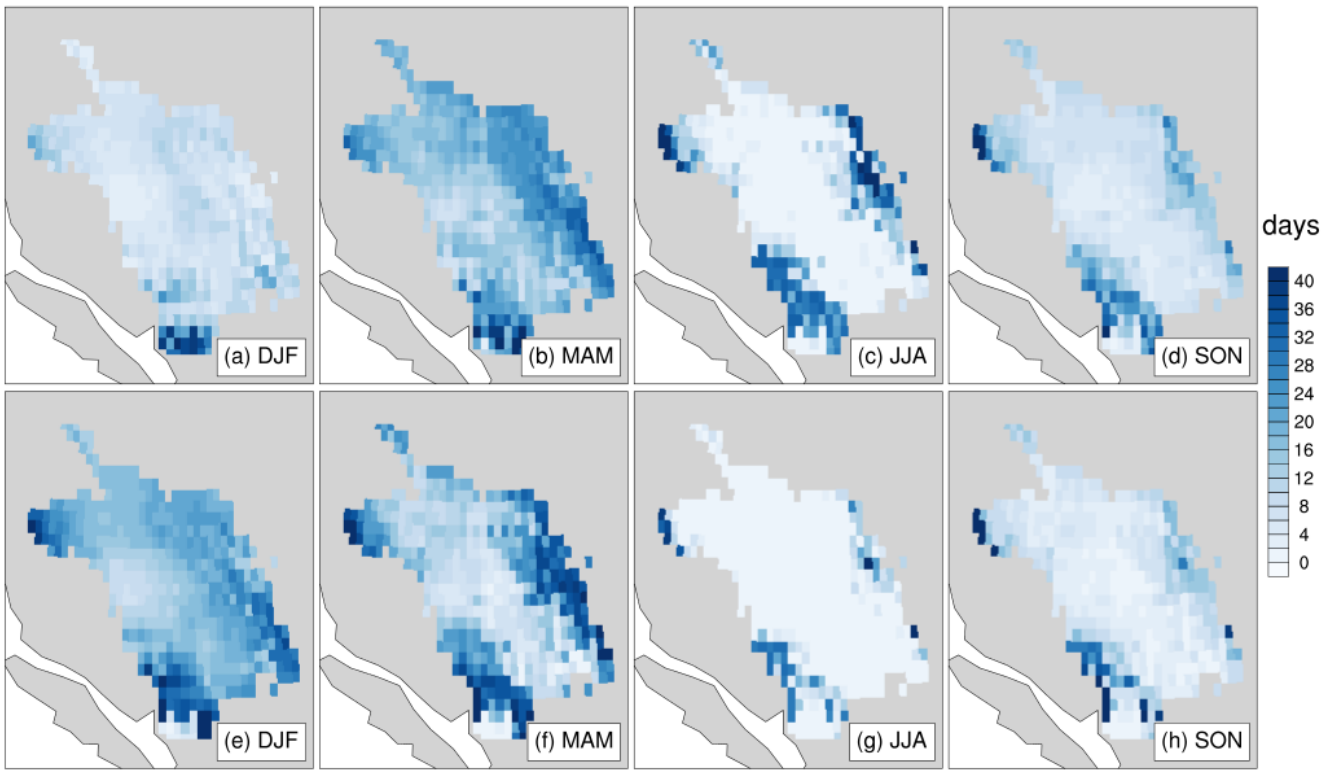

Figure 14: Comparison of the historical (top row) and scenario (bottom row) ROS events in the Fraser River Basin for different seasons (winter (DJF), spring (MAM), summer (JJA), and fall (SON)

The future change of the annual ROS events is further decomposed into Seasonal climatology of ROS events and compare the historical and scenario seasonal climatological trends. Comparing the historical and scenario ROS frequency in seasonal distribution, the early shifting of ROS intensity can be detected form spring to winter season which is a visible signal

of the ROS intensification in winter in future climate conditions. The entire basin is expected to receive a high frequency of the ROS in winter while only high elevated Coast and Rocky Mountains region is expected to receive a high frequency of ROS events in the future scenario. Similarly, the historic high frequency of ROS events in summer in both mountain ranges will not continue in the future and the only highly elevated region is expected to receive the ROS events which are limited by the snowpack availability on the surface in the summertime in future. In projection period, around 20 to 30 days of the winter ROS could be expected with the high frequency of ROS in Coast and Rocky regions and low in interior landmass while spring season has relatively less ROS events

As suggested in recent ROS studies (McCabe et al., 2007b; Surfleet & Tullos, 2013; Pradhanang et al., 2013a; Jeong & Sushama, 2017b), the future ROS evolution is examined in different elevation zones to characterize the elevation responses on the ROS evolution . The entire basin is split into different elevation zone of 500 meters interval to examine the ROS trend in different elevation ranges in the below section. Rapid warming (figure 8 (a)) and exceptionally high rainfall are observed in <500 m elevation zone (figure 12(a)) which motivates to split the basin area by 500 meters interval to examine the ROS frequency, mechanism and response to runoff.

3.4 Future Projected Changes of ROS Events

a) Elevation range 0 – 500 m

Below 500 m elevation comprises only the outlet portion of the FRB. The MME mean ROS events are expected to be 22 days in DJF season and 5 days in MAM on an average in the near-future with a higher range of model uncertainty. The winter ROS is expected to decrease continuously along with decreasing uncertainty at the end of the twenty-one century. In spring, only a few ROS events are expected in near future and this is not significant in the long-term future. There are no significant ROS events expected in summer and fall seasons in this elevation band (figure 15, panel (a)). The overall ROS event is sharply decreasing in 0 – 500 m elevation and expected rare ROS events in the winter season in the future. The seen in Figure 8(a), the warmer surface temperature has rapidly controlled the micro-climate condition which is not allowing snow on the surface. The lowest elevation zone will be the ROS free condition in the

future. The model uncertainty is much higher in the near term and gradually decreasing in the long-term future as most of the models are projecting the negative ROS in future.

b) Elevation range 501 – 1000 m

The MME mean ROS evolution trend is expected in the opposite of the lower elevation band. The winter ROS is projected to increase gradually from 13 days in near future to 20 days on average in the long-term future along with increasing uncertainty ranges. The spring ROS trend is expected in the opposite of DJF trend, decreasing from 16 days in near future to 10 days on average at the end of the 21st century. In SON, few numbers (6 days) of the ROS events are expected in near future with slightly decreasing trend in long-term while there are no ROS days detected in JJA in future (figure 15, panel (b)). In the elevation range of 501 – 1000 m, the winter and spring ROS are significantly high in number in all projection periods with slightly increasing winter ROS and slightly decreasing Spring ROS events in long term future. The overall ROS events in fairly remain the same in the 501 – 1000 m elevation zone. As the whisker of the boxplot is increasing in long-term future, higher model uncertainty is expected in long run.

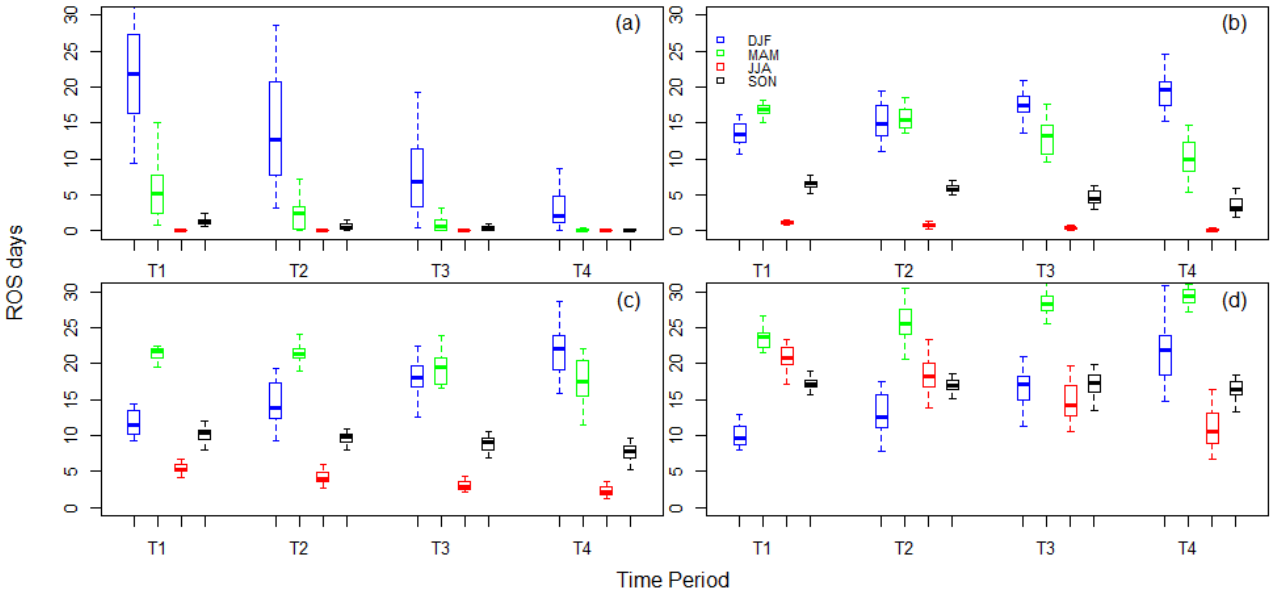

Figure 15: ROS distribution in Fraser Basin presented in multidecadal (T1=2020-2039, T2=2040-2059, T3=2060-2079, and T4=2080-2099), seasonal (DJF, MAM, JJA, and SON) and altitudinal distribution ((a)=0-500 m, (b)=501-1000 m, (c)=1001-1500 m and (d)=1500 & above m). Each boxplot length represents multi-model uncertainty and color indicates the season.

c) Elevation range 1001 – 1500 m

In the elevation band of 1001 to 1500 m, the MME mean ROS events are more frequent in all seasons where only DJF is expected to increase the number of events and the ROS days in other seasons are expected to slightly decrease from near future to long-term future. The ROS events in DJF are projected to double from 11 days in the near-term future to 21 days on average in the long-term future with continuously increasing model uncertainty ranges. The ROS event in summer season is significantly high number as compared with lower elevation zones. The ROS days in MAM season are expected to decrease from 21 to 17 days on average in the long-term future with increasing uncertainty. On average, 5 days of the ROS event is expected In JJA in near future which is subsequently decreasing in the long-term future. Additionally, the ROS days in SON season are expected to be 8 to 10 days which is a noticeable number as compared to lower elevation bands (figure. 15, panel (c)). Importantly, the winter ROS of this elevation zone is significantly increasing which could have potential implications in subsequent surface runoff. Overall the ROS event is expected to increase in 1001 – 1500 m elevation zone with higher numbers of ROS days in all seasons compared to lower elevation zones with associated increasing model uncertainty.

d) Elevation range 1501 m and above

In the highest elevation zone of 1501 m and above, the MME mean ROS events in all seasons are in significantly higher number. More importantly, the ROS tends in DJF is sharply increasing from 10 days to 22 days on average which shows the opposite trend of the lowest elevation band (0 to 500 m). the ROS days in MAM season show a significantly higher number in projection period compared to other seasons with slightly increasing from 24 days to 29 days on average from near to long-term future. The only decreasing ROS event is expected in JJA from 21 to 12 days on average while the ROS in SON remains constant around 12 days on an average. The overall high number of ROS events is expected in all seasons associated high model uncertainty in the projection of the ROS as the whisker of the boxplot is increasing in the long-term future.

3.5 Evaluation of ROS Events Simulation

a) Elevation range 0 - 500 m

As the response of rapidly increasing temperature and inversely decreasing snowpack in low elevation zone, the future ROS is sharply declining, and the ROS free condition is expected in the long-term future. The declining trend of the ROS is not only the response of SWE change or rainfall change, but it is likely dependent on temperature changes, the declining future ROS event is inversely correlated (R = -0.84) with the temperature changes in this low elevation zone. As a result of the minimum temperature exceeds the freezing point, the snowpack is not expected to be available to count the winter rainfall as the ROS event in the future. The ROS free condition in this region is the feedback of the aggressive temperature increase in the future.

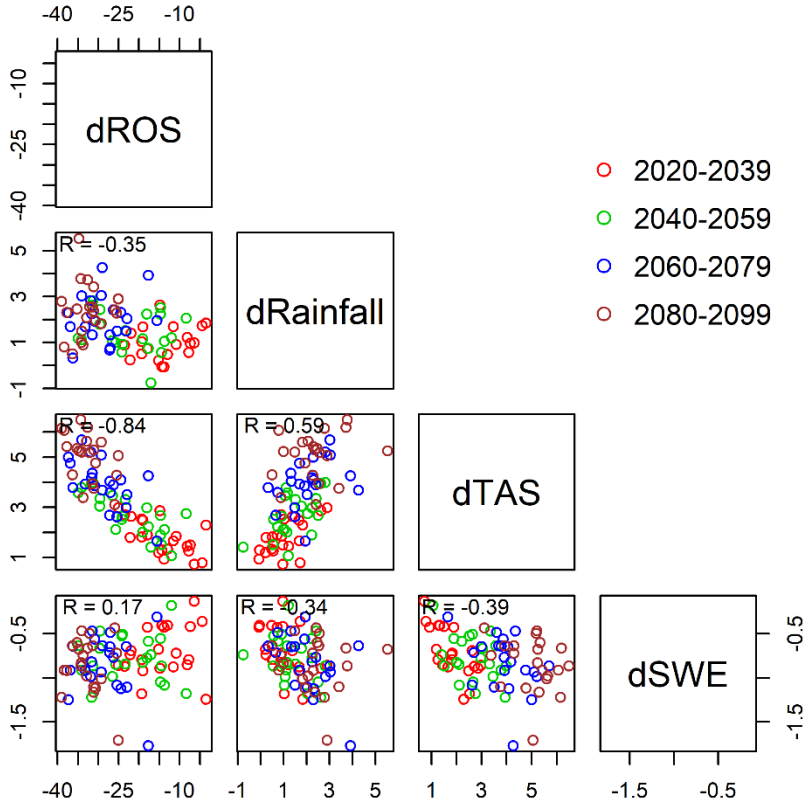

Figure 16: The association between projected change of ROS (dROS), Rainfall (dRainfall), Temperature (dTAS) and SWE (dSWE) in the elevation range of 0-500 m. Each circle represents one model projection, and the circle color indicates the time period.

b) Elevation range 501-1000 m

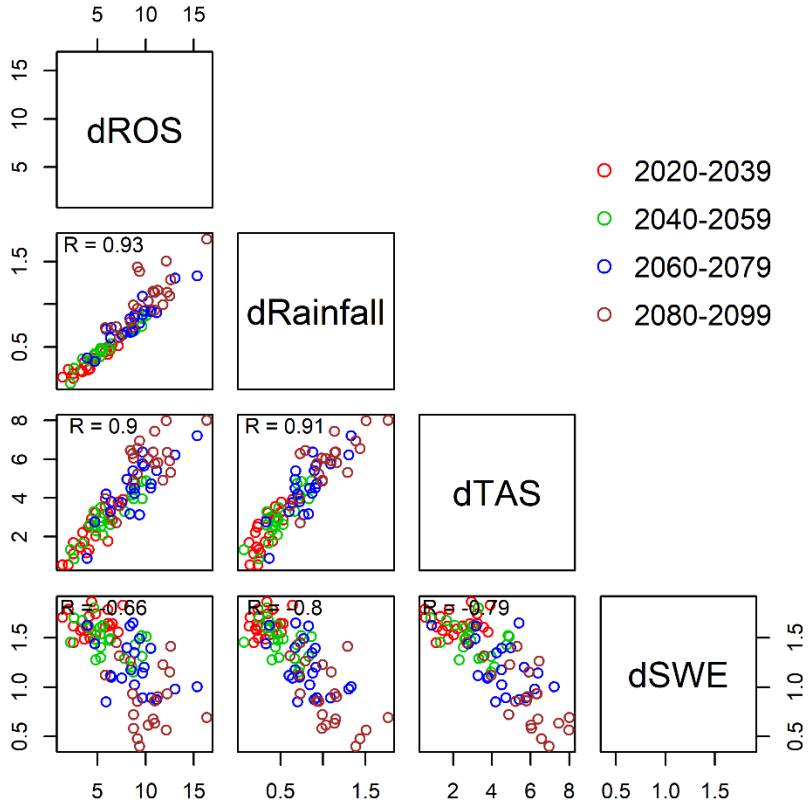

Figure 17: The association between dROS, dRainfall, dTAS and dSWE in the elevation range of 501-1000 m. Each circle represents one model projection, and the circle color indicates the time period.

Moving towards the middle range elevation zone (501 – 1000 m), the responses of temperature, and rainfall increment to the ROS evolution is different than the lowest elevation zone. As mentioned earlier in section 3.2.1, the temperature proximate towards 0℃ has a significant response to increasing the rain event and eventually to be counted as the ROS events. Even though the temperature and rainfall increasing and snowpack declining in higher elevation regions, there is still minimum snowpack available to be satisfied the condition of the ROS events up to the end of the twenty-first century. In the range of 501 to 1000 m elevations, the future evolution of the ROS evolution is highly correlated with both rainfall change (R=0.94) and temperature change (R=0.86), and the correlation is highly significant with the increasing trend of rainfall. As rain event increases in the cold season, the number of ROS events eventually increases. The increasing temperature and rainfall patterns are the major driving factors for the future ROS evolution in this elevation zone.

c) Elevation 1001 -1500 m

In the elevation range of 1001 -1500 m, the response of rainfall and temperature to the ROS evolution is highly significant. As mentioned above (section 3.2.1), the trend of temperature proximate toward 0℃ role to accelerate the rainfall events in the long-term future. The increasing temperature and rainfall have a positive response to the ROS evolution. The positive ROS evolution in this elevation zone is highly correlated with both rainfall (R=0.98) and temperature (R=0.95). As we move to a higher elevation region, snowpack resident time is longer and favors the condition of rainfall to be counted as the ROS events. The snowpack availability is not a limiting factor at all even though the snowpack is shrinking rapidly in the feedback of current climate. The accelerating ROS event has a potential response to speed up the melting process to even further declining the snowpack thickness in the long-term future.

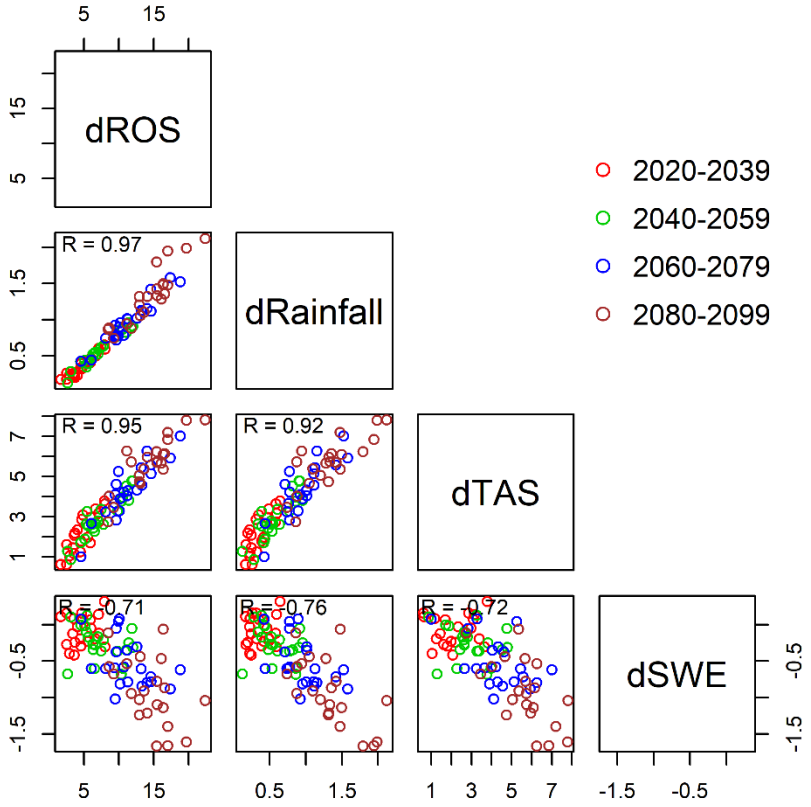

Figure18: The association between dROS, dRainfall, dTAS and dSWE in the elevation range of 1001-1500 m. Each circle represents one model projection, and the circle color indicates the time period.

d) Elevation 1501 m and above

In the highest elevation ranges of the FRB basin, the correlation of future ROS change with rainfall (R=0.98) and temperature (R=0.95) is significantly high. The rainfall and temperature change have major response on the ROS evolution in the highest elevation region as like the middle elevation regions. Similar to the middle ranges of elevation, SWE availability is not the limiting factor for the ROS evolution up to the end of the 21st century, even though the SWE is rapidly declining in this region too. In general, the ROS evolution is positive except <500 m elevation zone and highly increasing to the higher elevation zone in response to increasing temperature and rainfall events. The increasing rainfall and temperature are the major drivers for the positive ROS evolution in all three elevation zones except the elevation zone of <500 m. Again, the negative ROS evolution in elevation zone <500 is also a response of a rapidly warming temperature that does not favor snow accumulation on the ground.

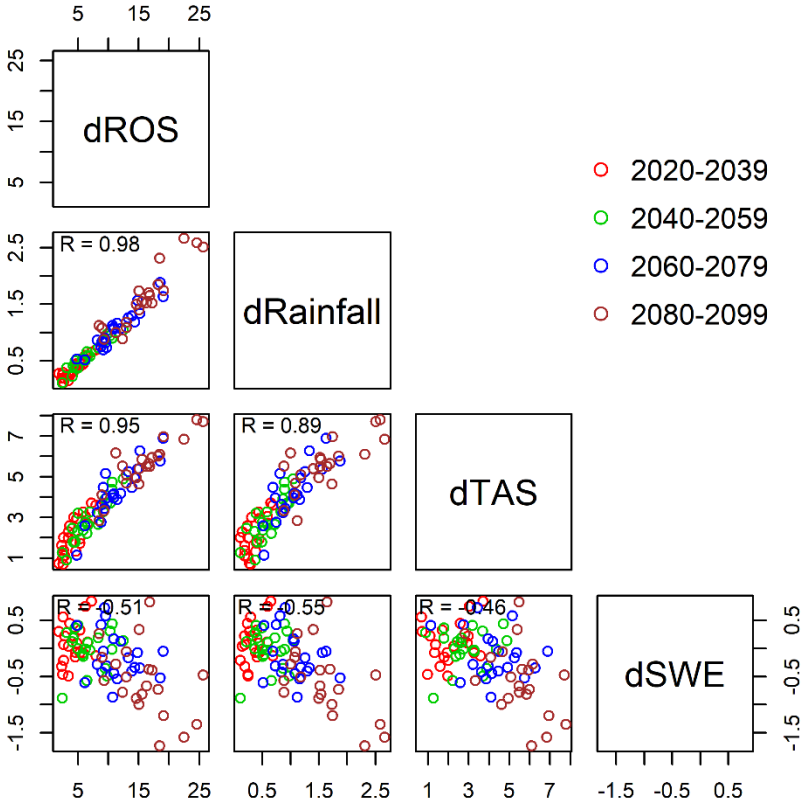

Figure 19: The association between dROS, dRainfall, dTAS and dSWE in the elevation range of 1501 m & above. Each circle represents one model projection, and the circle color indicates the time period.

3.6 ROS--Induced Runoff Changes

The impact of the ROS events on the surface runoff and associated streamflow has been documented in several rivers in cold region environments from West and East parts of North America, Northern Europe, Eurasia etc. Similarly, the FRB has been experiencing the high frequency of winter flooding (Rice et al., 2009; M. Schnorbus et al., 2010; Shrestha et al., 2012; Kang et al., 2014, 2016; Siraj U Islam et al., 2017; Curry & Zwiers, 2018) associated with the winter ROS-induced contribution. The impact of the ROS events on streamflow is different in different elevation regions.

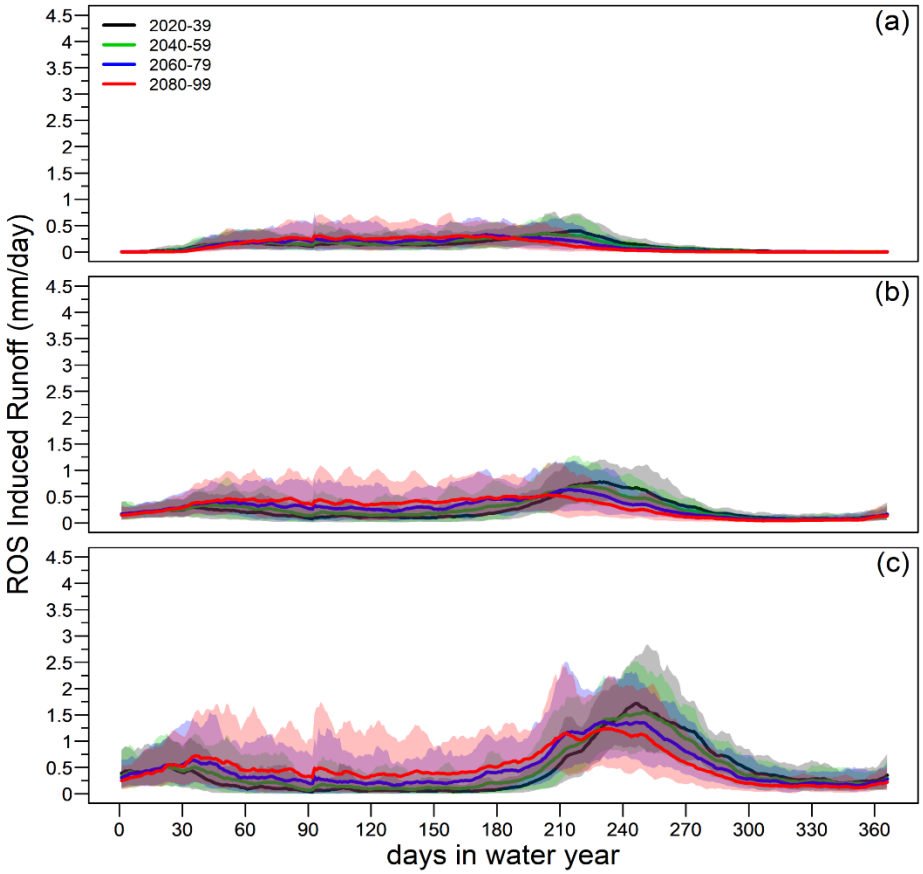

Figure 20: 7 days running average of ROS-induced spatial runoff in different period (indicated by color) in different elevation ranges, (a): 501 to 1000 m, (b): 1001 to 1500 m and (c): 1501 m & above with X-axis represent days in a year. The color indicates the time period.

The future ROS-induced runoff is expected to increase specifically in the middle and higher elevation zones. As the ROS frequency is rapidly declining in the lowest elevation zone (0 – 500 m) and its contribution to runoff is not noticeable in lowest elevation region (0 – 500 m) (figure

not shown) and it does not have impact to the entire watershed as the low elevated zone lies to the outlet portion of the basin. The increasing ROS frequency has a significant contribution to the runoff generation in the middle and higher elevation zones. Additionally, a relatively high and consistently longer period (Oct to April) of ROS-induced runoff is expected in the highest elevation region. In contrast to the lowest elevation zone, middle and higher ranges of elevation zones are expected to receive a significantly increased amount of the ROS-induced runoff in the long-term future. In the elevation zones of 501 to 1000 m, the winter ROS-induced runoff is expected to increase from 0.1mm/day in near future to 0.3 mm/day long term future while the total runoff is projected from 0.15 mm/day in near future to 0.5 mm/day in long term future. In 1001 to 1500 m, the winter ROS-induced runoff is projected from 0.2mm/day in near future to 0.45 mm/day in the long-term future while the total runoff is projected from 0.25 mm/day to 0.5 mm/day in long term future. Similarly, in 1501 m and above region, ROS-induced runoff is projected to increase consistently from 0.1 mm/day in near future to 0.5 mm/day in long term future with more ROS days in a year (Sept to July) while the total runoff is projected from 0.1 mm/day in near future to 0.6 mm/day in long term future. The ROS-induced runoff generation days varies depends on elevation range, shorter period (November to February) of the ROS-induced runoff contribution is expected in lower elevation region while the contribution period is gradually increasing (October to April) in higher elevation region. In all three elevation zones, the ROS event is projected to contribute around 50% of total surface runoff spatially in ROS active period.

The FRB is expected to receive consistently high flow throughout the winter season and peaks the runoff early spring season driven by temperature-induced snowmelt, increases in the mean rainfall and the ROS-induced snowmelt and subsequently decreasing the late spring minimum flow (Shrestha, Schnorbus, Werner, & Berland, 2012; Islam, Curry, Déry, & Zwiers, 2018) in future climate projection. The increasing surface runoff in the winter period is associated with the increased ROS trend potentially driven by warming temperature and increasing rainfall. Previous studies examined and discussed the signal of total runoff change, with highlighting the MME projected streamflow increases in cold months and peak flow is projected to shifting earlier in scenario (Kang, Gao, Shi, Islam, & Déry, 2016; Islam, Déry, & Werner, 2017; Islam, Curry, Déry, & Zwiers, 2018). Our result completely aligns with the previous study which clearly demonstrates consistently maintaining high runoff in cold months

and peak flow is projected to shift earlier. The ROS-induced runoff quantity is quite high in the high elevation region rather than the low elevation region. The high volume of the ROS-induced runoff generated at high elevation region has the potential to affect the lower elevation region as the runoff flows off to the downstream. The model uncertainty is represented by the ribbon of each color which is consistently high in long term future projection and in high elevation zone as well.

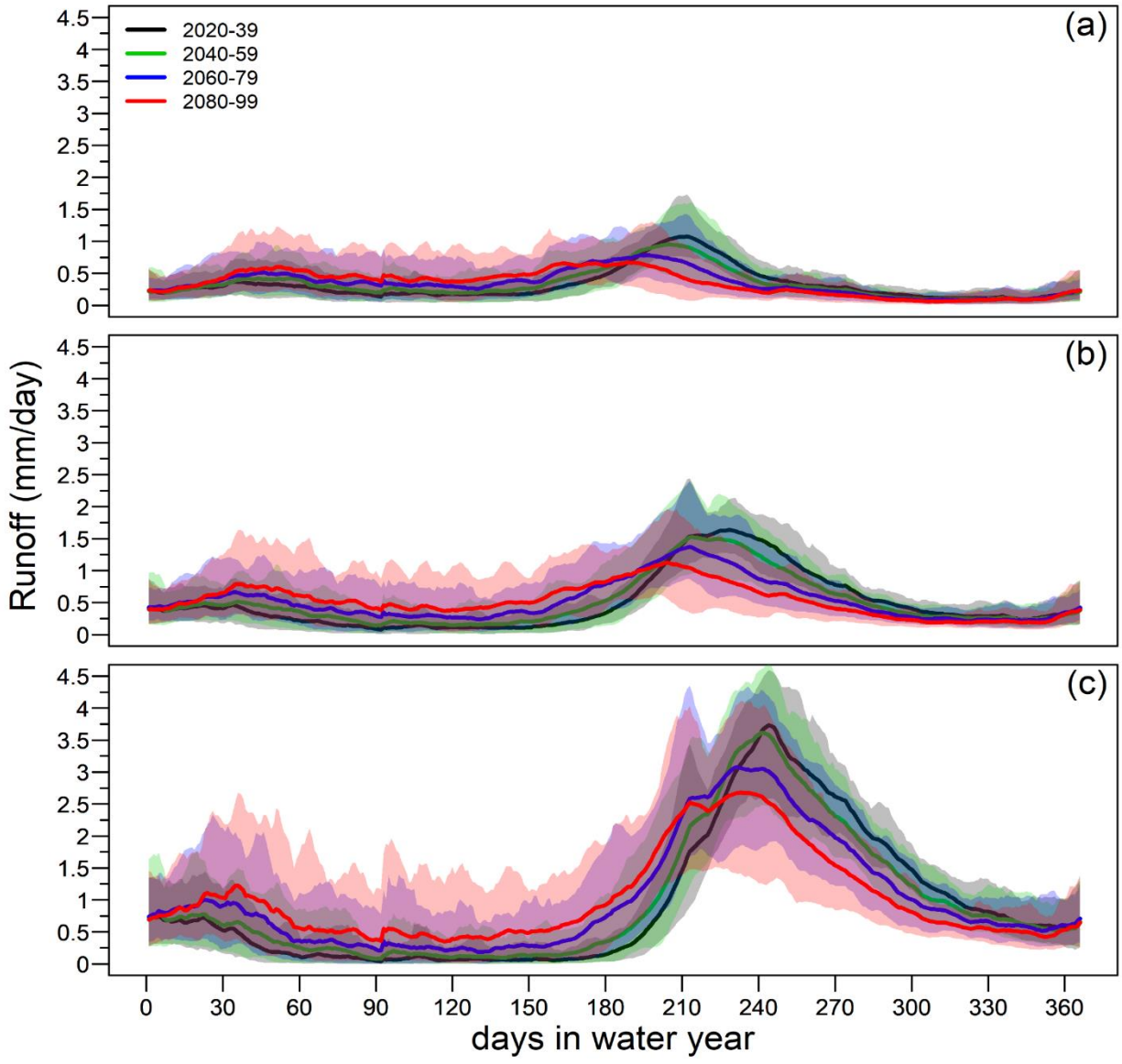

Figure 21: 7 days running average of spatial runoff in different period (indicated by color) in different elevation ranges, (a): 501 to 1000 m, (b): 1001 to 1500 m and (c): 1501 m & above with X-axis represent days in a year. The color indicates the time period.

Similar to the ROS-induced runoff, the total runoff generated in different elevational zones demonstrates that high elevation generates high total runoff with higher model uncertainty. The surface runoff in cold months is continuously increasing up to the end of the 21st century in all elevation zones along with the peak runoff time is expected to shift early spring. The ROS-induced runoff has a major contribution to increasing the total runoff in cold months in all elevation zones. In this ROS study, contribution of the ROS-induced runoff into the total runoff. The ROS-induced runoff significantly contributes ~50% portion of total runoff in cold seasons in all sub-regions. The future change in the ROS-induced runoff clearly demonstrates that a considerable fraction of the projected high total runoff in winter and early spring floods comes from ROS events in middle and higher elevation zones. The annual peak runoff for different projection periods demonstrates that both ROS-induced runoff and the total runoff are gradually early shifting in the long-term future from mid-spring to early spring. The winter ROS-induced runoff is consistently increasing from near to long term future in middle and high elevation ranges. As a result of winter ROS speeds up the snowmelt process and consistently maintaining high streamflow to downstream, eventually spring streamflow will be decreasing as most of the snowpack is already get melted with the impact of the ROS events. Previous research has detected a signal of climate change-induced hydrologic regime change in the FRB (Shrestha, Schnorbus, Werner, & Berland, 2012; Kang, Shi, Gao, & Déry, 2014; Islam & Déry, 2017; Islam, Déry, & Werner, 2017; Curry & Zwiers, 2018).

Chapter 4: Discussion

4.1 Future ROS Changes

The historical and scenario ROS events have been analyzed spatially and in different elevational zones. In observational analysis, high precipitation has been observed in the Coast and the Rocky mountains ranges (Shrestha et al., 2012), and the spatial ROS distribution trend in historical period has followed the precipitation pattern (Figure 6) in general, such as higher in the mountainous region and very low frequency in inner landmass where observed precipitation was very low. As the historical ROS distribution follows the precipitation pattern of high frequency in mountainous regions and low frequency in the inner part of the basin, snowpack availability is not a limiting factor for ROS events in cold seasons. The projected precipitation phase change in the Fraser River Basin is significantly a shift from solid to liquid precipitation with at least 40% less snowfall and subsequently increase rainfall events which is consistent with the results of previous studies in the basin (Kang, Gao, Shi, Islam, & Déry, 2016; Erler & Peltier, 2017; Islam, Déry, & Werner, 2017). The future ROS events has been expected to change with the different trends in different elevational zones in response of precipitation and temperature variabilities which has been observed to change across the basin with the influence of physiographic diversity (Shrestha, Schnorbus, Werner, & Berland, 2012; Kang, Shi, Gao, & Déry, 2014; Kang, Gao, Shi, Islam, & Déry, 2016; Islam, Déry, & Werner, 2017; Curry & Zwiers, 2018; Islam, Curry, Déry, & Zwiers, 2018). The precipitation increase in future is proximately 18 to 20 % annually with stronger increase in the Coast mountain range with low variability between ensemble members which is consistent with the result of (Erler & Peltier, 2017) and the ROS distributes following the precipitation trends with high frequency in east and west mountain ranges and low in frequency in larger area of interior landmass. This study provides new insight on the elevational response to ROS frequency distribution across the FRB.

The multidecadal and seasonal ROS distributions for short and long-term future demonstrate the different response of rainfall and temperature on future ROS events. The precipitation change (figure 10) and phase change (figure 11) under the projected warming of CMIP5 simulation, contributes to the declining snowpack accumulation in cold months (Islam, Curry, Déry, & Zwiers, 2018) and rapidly increasing the ROS events. As the total snowfall will convert

to rainfall (figure 11) in the lowest elevation band (<500m) which eventually results in the ROS free condition in this region in the future. The rapid declining of the ROS events in the future (which has the highest ROS frequency in number in the current climate) in <500 m will be limited by snowpack availability on the ground. In contrast with the lowest elevation band, the winter ROS days will increase in the future continuously in higher elevation bands, and the increment is even higher in the highest elevation ranges (>1501m). As the increasing temperature enhances the precipitation phase change (Kang et al., 2016) to increase the rainfall frequency in the cold season, on the other hand, even the snowpack is melting faster (Erler & Peltier, 2017), the snowpack will be remaining on the ground (Kang et al., 2016) to be counted the rainfall as the ROS events. Beyond the 21st century, there might be snowpack free condition up to lower altitude as the snowline moving upward in the response of increasing air temperature, and eventually brings the negative ROS events. At the highest elevation zone (>1501m), the ROS event is expected to receive throughout a year which indicates precipitation phase change strongly dominant in the cold season and annual snowpack will be remained up to 21st century to be satisfied as the ROS event, even though, the snowpack is rapidly shrinking over this period.

4.2 The mechanism driving future ROS evolution

The correlations of the ROS, rainfall, temperature and SWE for the multidecadal winter season were analyzed to characterize the responses of rainfall, temperature and SWE to the projected ROS events. These variables response differently to each elevation zone. In the <500m elevation, it is expected to be the ROS free winter in the future as the snowpack will not accumulate on the ground in response of rapid warming and 100% phase change of precipitation (Bawden et al., 2014; Erler & Peltier, 2016, 2017; Curry & Zwiers, 2018). The dROS is negatively correlated with the future rainfall and temperature change while it does not correlate with the declining SWE. The rapid declining ROS is not limited by the rainfall changes. The rapid declining trend of ROS is associated with the surface temperature change which does not favor snowfall and eventually snowpack decline on the earth's surface in the future period.

In contrast to the lowest elevation (<500m), the winter dROS in higher elevation ranges is continuously increasing. Both dRainfall and dTAS are strongly correlated with the dROS. The snowpack does sustain persistently for long term future in higher elevation regions even the snowpack depth is gradually shrinking in response to radiation and rain-induced melt (Kang et al., 2014, 2016). The dRainfall and dTAS have both a strong correlation with the dROS in higher

elevation regions. Even though the SWE is an important component to determine the rainfall as the ROS and the dSWE is decreasing continuously, but the declining SWE does not limit the ROS days as the remaining SWE is sufficiently available for the rainfall event to be counted as the ROS. Specifically, the increasing surface air temperature feedbacks to precipitation phase change to increase rainfall in the winter period result more positive ROS days in the future. The temperature-driven rainfall enhancement over the high elevation regions leads to a strong correlation with the ROS events. The snowpack availability can limit negative ROS when rapid shrinking is experienced beyond the 21st century with an ongoing warming trend.

Additionally, the minimum temperature density distribution in the multi-decadal trend demonstrates the continuous increment of the positive feedback (figure 9) to the ROS evolution on the basin average. The density distribution of minimum temperature in the FRB shows that the peak density is continuously moving towards 0℃ which could create rain favorable conditions and eventually responses to higher ROS events in long term future. The minimum temperature density distribution clearly demonstrates the higher probability of the minimum temperature close to 0℃ in long term future which could create a condition to be counted as the rainfall as the ROS event. The monotonically shifting the minimum temperature towards to positive number illustrates the response of changing temperature in the future ROS evolution.

4.3 ROS Responses to Runoff

In general, cold season runoff is increasing in FRB continuously. As climate warming, the spring peak runoff is expected to shift earlier in early spring period along with consistently high runoff throughout the winter season in long term future (Kang, Gao, Shi, Islam, & Déry, 2016; Islam, Déry, & Werner, 2017; Islam, Curry, Déry, & Zwiers, 2018). The increasing winter ROS event has a significant contribution to the total runoff in the winter season. The winter runoff is projected to consistently increase with the early shifting of spring freshet peak flow which is consistent with the previous researches from Islam, Déry, & Werner (2017); Curry & Zwiers (2018). The ROS-induced runoff contributes to the total runoff in the cold season and the contribution trend is expected to increase continuously up to the end of the 21st century, shared about 50% out of the total runoff. The ROS accelerates the surface runoff by melting the snowpack on the ground and eventually limiting spring freshet with sharply declining spring flow. The projection of ROS event increases continuously in high elevation corresponds with the increasing ROS runoff in higher elevations in the long-term future. In a basin scale, the ROS

event shifts seasonal hydrologic regime with changing flow levels, i.e. increasing flow in the cold season, earlier shifting the peak flow to early spring, and subsequently sharp decline spring flow. The shifting in hydrologic regime can impact on several sectors to downstream water users such as dam operation for hydropower, irrigation, municipal supply, transportation, ecology, fisheries, etc. The annual hydrologic pattern of the basin could be shifted from low winter flow to consistently high winter flow, freshet flood in late spring to moderate flood in early spring and sustaining spring flow to shallow spring flow. This study reveals that a warming climate results in significant changes in hydrologic regime of the FRB. Indeed, the winter runoff in future will be contributed by the ROS-induced runoff consistently and the contribution is seemed to be much stronger in the long-term future in higher elevation region. This research adds to the existing recent literatures which highlight the winter flow increasing along with early shifting of peak flow timing (Islam, Déry, & Werner, 2017; Islam, Curry, Déry, & Zwiers, 2018) by quantifying the contribution of ROS-induced runoff into the total runoff. This research additionally explores the total runoff and the ROS-induced runoff in different elevation zones which gives further insight of elevational response to generate surface runoff in future. From the perspective of water resource management, there will be a more challenge to manage water demand in the future. The ROS-induced enhanced streamflow in the winter season could be regulated and utilized in spring season while water demand would be high and natural streamflow would be low. The FRB is a hotspot for the pacific salmon breeding demanding high spring flow to migrate fish toward the upstream region (Schnorbus, Werner, & Bennett, 2010) while the ROS events could diminish the streamflow in the spring in the long-term future. The regulating the ROS-induced runoff in winter season and releasing in the spring season would be a potential adaptation to management the water demand for economic and ecological consumption in future. The novel contribution of this research is to highlight the ROS evolution and the ROS-induced runoff contribution across the elevation to the total runoff in the future.

Chapter 5: Conclusion

5.1 Summary

This thesis analyzed the historical and future evolution of the ROS event in the Fraser River Basin using observed and global climate model data. The result presented in chapter 3 discusses the historical trend and scenario trend of ROS distribution in different seasonality in different elevation ranges. The temperature and rainfall response on the ROS evolution are presented with respect to seasonality and elevations. The future ROS evolution is greatly varying on different elevation ranges in different seasons. The variation of the ROS events has been generally influenced by both rainfall and the warming temperature trend. Even though some ROS events have been observed in all seasons, our study has been focused on the winter ROS event and its subsequent impact on changes surface runoff to downstream. The model uncertainty of ROS was assessed using a multi-model which shown as a spread of plot.

In the lowest elevation zone, air temperature is normally warm enough which is not favorable for winter snow accumulation for the long-term future. Different than the lower elevation zone, air temperature in higher elevation is less than the freezing line in current climate conditions and gradually warming up proximate towards to melting point which creates a favorable condition to turn the precipitation as rainfall.

Along with warming air temperature, the frequency of rainfall is increasing in mid and high elevation zones of the FRB region. The increasing frequency of winter rainfall has a significant contribution to increasing the ROS events in the winter season in high elevation ranges where the longer resident snowpack is available. In the elevation zone below 500 m, ROS events are projected to decline dramatically such that by 2100 they may cease to occur regularly in the FRB. In the elevation zones above 500 m, ROS events are projected to increase with elevation from the near future to long term future where the temperature and rainfall changes are positive and outweigh SWE reductions. Even though the snowpack is shrinking rapidly at these elevations, sufficient snow is projected to remain to sustain frequent ROS events.

The projected increase in the frequency of ROS events at higher elevation zones in long term future has a direct contribution to the surface runoff in winter and subsequent spring seasons. It is expected to enhance winter runoff contributing up to 50% of total winter runoff and sharply declining spring runoff driven by ROS-induced snowpack melt. The evaluation of the ROS helps

to understand hydroclimatic regime changes in Fraser River Basin and it can provide new insights into how the winter snowpack shrinking rapidly in the response of the ROS events and changing flow regime with high flow in winter and subsequent low flow in the spring period. The ROS evaluation result can be useful for water resources professionals to capture the moderately high winter flow in a reservoir to maintain spring flow when freshwater demand is high for economic and ecological supply. The overall results of the ROS analysis suggest that a similar method of hydro-climatic analysis using the ROS event counting could be implemented over other watersheds in high latitude regions to provide insight about climate change impact in hydro-climatic regime.

References

Balsamo, G., Albergel, C., Beljaars, A., Boussetta, S., Brun, E., Cloke, H., … Vitart, F. (2015). ERA-Interim/Land: A global land surface reanalysis data set. *Hydrology and Earth System Sciences*, *19*(1), 389–407. https://doi.org/10.5194/hess-19-389-2015

Barnett, T. P., Pierce, D. W., Hidalgo, H. G., Bonfils, C., Santer, B. D., Das, T., … Dettinger, M. D. (2008). Human-Induced Changes in the Hydrology of the Western United States. *Science*, *319*(5866), 1080–1083. https://doi.org/10.1126/science.1152538

Bawden, A. J., Linton, H. C., Burn, D. H., & Prowse, T. D. (2014). A spatiotemporal analysis of hydrological trends and variability in the Athabasca River region, Canada. *Journal of Hydrology*, *509*, 333–342. https://doi.org/10.1016/j.jhydrol.2013.11.051

Bonfils, C., Santer, B. D., Pierce, D. W., Hidalgo, H. G., Bala, G., Das, T., … Nozawa, T. (2008). Detection and Attribution of Temperature Changes in the Mountainous Western United States. *Journal of Climate*, *21*(23), 6404–6424. https://doi.org/10.1175/2008JCLI2397.1

Brun, E., Vionnet, V., Boone, A., Decharme, B., Peings, Y., Valette, R., … Morin, S. (2012). Simulation of Northern Eurasian Local Snow Depth, Mass, and Density Using a Detailed Snowpack Model and Meteorological Reanalyses. *Journal of Hydrometeorology*, *14*(1), 203–219. https://doi.org/10.1175/JHM-D-12-012.1

Cohen, J., Ye, H., & Jones, J. (2015). Trends and variability in rain-on-snow events. *Geophysical Research Letters*, *42*(17), 2015GL065320. https://doi.org/10.1002/2015GL065320

Curry, C. L., & Zwiers, F. W. (2018). Examining controls on peak annual streamflow and floods in the Fraser River Basin of British Columbia. *Hydrology and Earth System Sciences*, *22*(4), 2285–2309. https://doi.org/10.5194/hess-22-2285-2018

Déry, S. J., Stahl, K., Moore, R. D., Whitfield, P. H., Menounos, B., & Burford, J. E. (2009). Detection of runoff timing changes in pluvial, nival, and glacial rivers of western Canada:

WESTERN CANADA RUNOFF TIMING. *Water Resources Research*, *45*(4). https://doi.org/10.1029/2008WR006975

Dumanski, S., Pomeroy, J. W., & Westbrook, C. J. (2015). Hydrological regime changes in a Canadian Prairie basin. *Hydrological Processes*, *29*(18), 3893–3904. https://doi.org/10.1002/hyp.10567

Erler, A. R., & Peltier, W. R. (2016). Projected Changes in Precipitation Extremes for Western Canada based on High-Resolution Regional Climate Simulations. *Journal of Climate*, *29*(24), 8841–8863. https://doi.org/10.1175/JCLI-D-15-0530.1

Erler, A. R., & Peltier, W. R. (2017). Projected Hydroclimatic Changes in Two Major River Basins at the Canadian West Coast Based on High-Resolution Regional Climate Simulations. *Journal of Climate*, *30*(20), 8081–8105. https://doi.org/10.1175/JCLI-D-16-0870.1

Fleming, S. W., & Weber, F. A. (2012). Detection of long-term change in hydroelectric reservoir inflows: Bridging theory and practise. *Journal of Hydrology*, *470–471*, 36–54. https://doi.org/10.1016/j.jhydrol.2012.08.008

Gao, H., Tang, Q., Shi, X., Zhu, C., Bohn, T., Su, F., … Wood, E. F. (2010). *Water Budget Record from Variable Infiltration Capacity (VIC) Model*. Retrieved from http://eprints.lancs.ac.uk/89407/1/Gao_et_al_VIC_2014.pdf

Garvelmann, J., Pohl, S., & Weiler, M. (2015). Spatio-temporal controls of snowmelt and runoff generation during rain-on-snow events in a mid-latitude mountain catchment. *Hydrological Processes*, *29*(17), 3649–3664. https://doi.org/10.1002/hyp.10460

Gray, C. B. J., Tuominen, T. M., & Fraser River Action Plan (Canada). (1999). *Health of the Fraser River aquatic ecosystem: A synthesis of research conducted under the Fraser River Action Plan*. Vancouver: Fraser River Action Plan.

Graybeal, D. Y., & Leathers, D. J. (2006). Snowmelt-related flood risk in Appalachia: First estimates from a historical snow climatology. *Journal of Applied Meteorology and Climatology*, *45*(1), 178–193.

Hatcher, K. L., & Jones, J. A. (2013). Climate and Streamflow Trends in the Columbia River Basin: Evidence for Ecological and Engineering Resilience to Climate Change. *Atmosphere-Ocean*, *51*(4), 436–455. https://doi.org/10.1080/07055900.2013.808167

Huntington, T. G., Hodgkins, G. A., Keim, B. D., & Dudley, R. W. (2004). Changes in the proportion of precipitation occurring as snow in New England (1949–2000). *Journal of Climate*, *17*(13), 2626–2636.

Hutchinson, M. F., McKenney, D. W., Lawrence, K., Pedlar, J. H., Hopkinson, R. F., Milewska, E., & Papadopol, P. (2009). Development and Testing of Canada-Wide Interpolated Spatial Models of Daily Minimum–Maximum Temperature and Precipitation for 1961–2003: Journal of Applied Meteorology and Climatology: Vol 48, No 4. Retrieved August 20, 2019, from https://journals.ametsoc.org/doi/full/10.1175/2008JAMC1979.1

IPCC. (2013). *Summary for Policymakers. In: Climate Change 2013: The Physical Science Basis. Contribution of Working Group I to the Fifth Assessment Report of the Intergovernmental Panel on Climate Change [Stocker, T.F., D. Qin, G.-K. Plattner, M. Tignor, S.K. Allen, J. Boschung, A. Nauels, Y. Xia, V. Bex and P.M. Midgley (eds.)]*. Cambridge University Press, Cambridge, United Kingdom and New York, NY, USA.

IPCC (Ed.). (2014). *Climate Change 2014: Synthesis Report. Contribution of Working Groups I, II and III to the Fifth Assessment Report of the Intergovernmental Panel on Climate Change [Core Writing Team, R.K. Pachauri and L.A. Meyer (eds.)]*. Geneva, Switzerland: Intergovernmental Panel on Climate Change.

Islam, Siraj U, Déry, S. J., & Werner, A. T. (2017). Future Climate Change Impacts on Snow and Water Resources of the Fraser River Basin, British Columbia. *Journal of Hydrometeorology*, *18*(2), 473–496. https://doi.org/10.1175/JHM-D-16-0012.1

Islam, Siraj Ul, Curry, C. L., Déry, S. J., & Zwiers, F. W. (2018). Quantifying projected changes in runoff variability and flow regimes of the Fraser River Basin, British Columbia. *Hydrology and Earth System Sciences Discussions*, 1–44. https://doi.org/10.5194/hess-2018-232

Islam, Siraj Ul, & Déry, S. J. (2017). Evaluating uncertainties in modelling the snow hydrology of the Fraser River Basin, British Columbia, Canada. *Hydrology and Earth System Sciences*, *21*(3), 1827–1847. https://doi.org/10.5194/hess-21-1827-2017

Jeong, D. I., & Sushama, L. (2017). Rain-on-snow events over North America based on two Canadian regional climate models. *Climate Dynamics*. https://doi.org/10.1007/s00382-017-3609-x

Kang, D. H., Gao, H., Shi, X., Islam, S. ul, & Déry, S. J. (2016). Impacts of a Rapidly Declining Mountain Snowpack on Streamflow Timing in Canada's Fraser River Basin. *Scientific Reports*, *6*(1). https://doi.org/10.1038/srep19299

Kang, D. H., Shi, X., Gao, H., & Déry, S. J. (2014). On the Changing Contribution of Snow to the Hydrology of the Fraser River Basin, Canada. *Journal of Hydrometeorology*, *15*(4), 1344–1365. https://doi.org/10.1175/JHM-D-13-0120.1

Liang, X., Lettenmaier, D. P., Wood, E. F., & Burges, S. J. (1994). A simple hydrologically based model of land surface water and energy fluxes for general circulation models. *Journal of Geophysical Research: Atmospheres*, *99*(D7), 14415–14428. https://doi.org/10.1029/94JD00483

Liang, X., Wood, E. F., & Lettenmaier, D. P. (1996). Surface soil moisture parameterization of the VIC-2L model: Evaluation and modification. *Global and Planetary Change*, *13*(1), 195–206. https://doi.org/10.1016/0921-8181(95)00046-1

Mazurkiewicz, A. B., Callery, D. G., & McDonnell, J. J. (2008). Assessing the controls of the snow energy balance and water available for runoff in a rain-on-snow environment. *Journal of Hydrology*, *354*(1–4), 1–14. https://doi.org/10.1016/j.jhydrol.2007.12.027

McCabe, G. J., Hay, L. E., & Clark, M. P. (2007a). Rain-on-Snow Events in the Western United States. *Bulletin of the American Meteorological Society*, *88*(3), 319–328. https://doi.org/10.1175/BAMS-88-3-319

McCabe, G. J., Hay, L. E., & Clark, M. P. (2007b). Rain-on-Snow Events in the Western United States. *Bulletin of the American Meteorological Society*, *88*(3), 319–328. https://doi.org/10.1175/BAMS-88-3-319

Mudryk, L. R., Derksen, C., Kushner, P. J., & Brown, R. (2015). Characterization of Northern Hemisphere Snow Water Equivalent Datasets, 1981–2010. *Journal of Climate*, *28*(20), 8037–8051. https://doi.org/10.1175/JCLI-D-15-0229.1

Musselman, K. N., Lehner, F., Ikeda, K., Clark, M. P., Prein, A. F., Liu, C., … Rasmussen, R. (2018). Projected increases and shifts in rain-on-snow flood risk over western North America. *Nature Climate Change*, *8*(9), 808. https://doi.org/10.1038/s41558-018-0236-4

Nijssen, B., Lettenmaier, D. P., Liang, X., Wetzel, S. W., & Wood, E. F. (1997). Streamflow simulation for continental-scale river basins. *Water Resources Research*, *33*(4), 711–724. https://doi.org/10.1029/96WR03517

Pierce, D. W., Barnett, T. P., Hidalgo, H. G., Das, T., Bonfils, C., Santer, B. D., … Nozawa, T. (2008). Attribution of Declining Western U.S. Snowpack to Human Effects. *Journal of Climate*, *21*(23), 6425–6444. https://doi.org/10.1175/2008JCLI2405.1

Pomeroy, J. W., Fang, X., & Marks, D. G. (2016). The cold rain-on-snow event of June 2013 in the Canadian Rockies - characteristics and diagnosis: The Cold Rain-on-Snow Event of June 2013 in the Canadian Rockies. *Hydrological Processes*, *30*(17), 2899–2914. https://doi.org/10.1002/hyp.10905

Pradhanang, S. M., Frei, A., Zion, M., Schneiderman, E. M., Steenhuis, T. S., & Pierson, D. (2013). Rain-on-snow runoff events in New York: RAIN-ON-SNOW EVENTS IN NEW YORK. *Hydrological Processes*, *27*(21), 3035–3049. https://doi.org/10.1002/hyp.9864

Putkonen, J., & Roe, G. (2003). Rain-on-snow events impact soil temperatures and affect ungulate survival: RAIN-ON-SNOW EVENTS IMPACT SOIL TEMPERATURES. *Geophysical Research Letters*, *30*(4). https://doi.org/10.1029/2002GL016326

Putnam, A. E., & Broecker, W. S. (2017). Human-induced changes in the distribution of rainfall. *Science Advances*, *3*(5), e1600871. https://doi.org/10.1126/sciadv.1600871

Rice, S. P., Church, M., Wooldridge, C. L., & Hickin, E. J. (2009). Morphology and evolution of bars in a wandering gravel-bed river; lower Fraser river, British Columbia, Canada. *Sedimentology*, *56*(3), 709–736. https://doi.org/10.1111/j.1365-3091.2008.00994.x

Rienecker, M. M., Suarez, M. J., Gelaro, R., Todling, R., Bacmeister, J., Liu, E., … Woollen, J. (2011). MERRA: NASA's Modern-Era Retrospective Analysis for Research and Applications. *Journal of Climate*, *24*(14), 3624–3648. https://doi.org/10.1175/JCLI-D-11-00015.1

Rodell, M., Houser, P. R., Jambor, U., Gottschalck, J., Mitchell, K., Meng, C.-J., … Toll, D. (2004). The Global Land Data Assimilation System. *Bulletin of the American Meteorological Society*, *85*(3), 381–394. https://doi.org/10.1175/BAMS-85-3-381

Schnorbus, M. A., & Cannon, A. J. (2014). Statistical emulation of streamflow projections from a distributed hydrological model: Application to CMIP3 and CMIP5 climate projections for British Columbia, Canada. *Water Resources Research*, *50*(11), 8907–8926. https://doi.org/10.1002/2014WR015279

Schnorbus, M., Werner, A., & Bennett, K. (2010). *Quantifying the water resource impacts of mountain pine beetle and associated salvage harvest operations across a range of watershed scales: Hydrologic modelling of the Fraser River Basin*. Victoria, B.C: Natural Resources Canada, Canadian Forest Service, Pacific Forestry Centre.

Schnorbus, M., Werner, A., & Bennett, K. (2014). Impacts of climate change in three hydrologic regimes in British Columbia, Canada. *Hydrological Processes*, *28*(3), 1170–1189. https://doi.org/10.1002/hyp.9661

Shrestha, R. R., Schnorbus, M. A., Werner, A. T., & Berland, A. J. (2012). Modelling spatial and temporal variability of hydrologic impacts of climate change in the Fraser River basin, British Columbia, Canada. *Hydrological Processes*, *26*(12), 1840–1860. https://doi.org/10.1002/hyp.9283

Singh, P., Spitzbart, G., Hübl, H., & Weinmeister, H. W. (1997). Hydrological response of snowpack under rain-on-snow events: A field study. *Journal of Hydrology*, *202*(1), 1–20. https://doi.org/10.1016/S0022-1694(97)00004-8

Sturm, M., Goldstein, M. A., & Parr, C. (2018). Water and life from snow: A trillion dollar science question. *Reviews of Geophysics*, 3534–3544. https://doi.org/10.1002/2017WR020840@10.1002/(ISSN)1944-9208.COMHES1

Surfleet, C. G., & Tullos, D. (2013). Variability in effect of climate change on rain-on-snow peak flow events in a temperate climate. *Journal of Hydrology*, *479*, 24–34. https://doi.org/10.1016/j.jhydrol.2012.11.021

Takala, M., Luojus, K., Pulliainen, J., Derksen, C., Lemmetyinen, J., Kärnä, J.-P., … Bojkov, B. (2011). Estimating northern hemisphere snow water equivalent for climate research through assimilation of space-borne radiometer data and ground-based measurements. *Remote Sensing of Environment*, *115*(12), 3517–3529. https://doi.org/10.1016/j.rse.2011.08.014

Taylor, K. E., Stouffer, R. J., & Meehl, G. A. (2012). An Overview of CMIP5 and the Experiment Design. *Bulletin of the American Meteorological Society*, *93*(4), 485–498. https://doi.org/10.1175/BAMS-D-11-00094.1

UNBC study warns of future flooding in Fraser River basin. (2019, March 4). Retrieved March 6, 2019, from CKPGToday website: https://ckpgtoday.ca/article/554591/unbc-study-warns-future-flooding-fraser-river-basin

Wade, N. L., Martin, J., & Whitfield, P. H. (2001). Hydrologic and Climatic Zonation of Georgia Basin, British Columbia. *Canadian Water Resources Journal / Revue Canadienne Des Ressources Hydriques*, *26*(1), 43–70. https://doi.org/10.4296/cwrj2601043

Wayand, N. E., Clark, M. P., & Lundquist, J. D. (2017). Diagnosing snow accumulation errors in a rain-snow transitional environment with snow board observations: Diagnosing Snow Accumulation Errors. *Hydrological Processes*, *31*(2), 349–363. https://doi.org/10.1002/hyp.11002

Wen, Z., Liang, X., & Yang, S. (2012). A new multiscale routing framework and its evaluation for land surface modeling applications. *Water Resources Research*, *48*(8). https://doi.org/10.1029/2011WR011337

Winter wallop: Heavy snow, rain hammer southern B.C. | CTV News. (2018, December 18). Retrieved February 5, 2019, from https://bc.ctvnews.ca/winter-wallop-heavy-snow-rain-hammer-southern-b-c-1.4223238

Ye, H., Yang, D., & Robinson, D. (2008). Winter rain on snow and its association with air temperature in northern Eurasia. *Hydrological Processes*, *22*(15), 2728–2736. https://doi.org/10.1002/hyp.7094

Appendix

Table 1: List of the 21 CMIP5 models used in the present study

Institution	Model Name
Commonwealth Scientific and Industrial Research Organization (CSIRO) and Bureau of Meteorology (BOM), Australia	ACCESS1-0 ACCESS1-3
Beijing Climate Center, China Meteorological Administration	bcc-csm1-1 bcc-csm1-1-m
College of Global Change and Earth System Science, Beijing Normal University, China	BNU-ESM
Canadian Centre for Climate Modelling and Analysis, Canada	CanESM2
National Center for Atmospheric Research, U.S.A.	CCSM4
Centre National de Recherches Météorologiques/Centre Européen de Recherche et Formation Avancée en Calcul Scientifique, France	CNRM-CM5
Commonwealth Scientific and Industrial Research Organization in collaboration with Queensland Climate Change Centre of Excellence, Australia	CSIRO-Mk3-6-0
LASG, Institute of Atmospheric Physics, Chinese Academy of Sciences; and CESS, Tsinghua University, China	FGOALS-g2
NOAA Geophysical Fluid Dynamics Laboratory, U.S.A.	GFDL-CM3 GFDL-ESM2G GFDL-ESM2M
Institute for Numerical Mathematics, Russia	inmcm4
Institut Pierre-Simon Laplace, France	IPSL-CM5A-LR
Japan Agency for Marine-Earth Science and Technology, Atmosphere and Ocean Research Institute and National Institute for Environmental Studies, Japan	MIROC5 MIROC-ESM
Max Planck Institute for Meteorology, Germany	MPI-ESM-LR MPI-ESM-MR
Meteorological Research Institute, Japan	MRI-CGCM3
Norwegian Climate Centre, Norway	NorESM1-M